Review Article

Nano Research
2024, 17(2): 426–444

ISSN 1998-0124 CN 11-5974/O4
https://doi.org/10.1007/s12274-023-5606-1

Organic thin-film transistors and related devices in life and health monitoring

Chenfang Sun (✉) and Tie Wang (✉)

Tianjin Key Laboratory of Drug Targeting and Bioimaging, Life and Health Intelligent Research Institute, Tianjin University of Technology, Tianjin 300384, China

Received: 26 December 2022 / **Revised:** 21 February 2023 / **Accepted:** 22 February 2023

ABSTRACT

The early determination of disease-related biomarkers can significantly improve the survival rate of patients. Thus, a series of explorations for new diagnosis technologies, such as optical and electrochemical methods, have been devoted to life and health monitoring. Organic thin-film transistor (OTFT), as a state-of-the-art nano-sensing technology, has attracted significant attention from construction to application owing to the merits of being label-free, low-cost, facial, and rapid detection with multi-parameter responses. Nevertheless, interference from non-specific adsorption is inevitable in complex biological samples such as body liquid and exhaled gas, so the reliability and accuracy of the biosensor need to be further improved while ensuring sensitivity, selectivity, and stability. Herein, we overviewed the composition, mechanism, and construction strategies of OTFTs for the practical determination of disease-related biomarkers in both body fluids and exhaled gas. The results show that the realization of bio-inspired applications will come true with the rapid development of high-effective OTFTs and related devices.

KEYWORDS

organic thin-film transistors, biosensors, biomarkers, organic bioelectronics, organic semiconductors, healthcare

1 Introduction

The early diagnosis of diseases is closely related to the life and health of people, so it is crucial to develop a simple, rapid, and accurate method for ultra-early disease diagnosis with high reliability and accuracy. As a typical product of cross-fertilization, biosensors [1] span multiple disciplines, including chemical science, material science, physical science, life science, and information science. Generally speaking, biosensors consisting of sensitive probes and converters can transfer the measured information into electrical or other desired signals according to specific laws. The detection of target analytes can be divided into three processes: target identification, signal conversion, and signal output. For instance, when the target analyte interacts with the sensitive probes on the sensing surface, the chemical, physical, and biological signals are recognized by the biosensors and then converted into a readable output signal to achieve specific identification. The research for biosensors not only introduces the latest achievements in material science into biomedical applications, but also transplants life science into information science to provide new methods for information transfer and storage. Among them, biosensors based on organic thin-film transistors (OTFTs) [2, 3] with small size, high precision, and good performance can significantly enrich the theory and broaden the application field of biosensors. Compared with traditional techniques, such as optical and electrochemical methods, OTFT-based biosensors [4–7] have more unique advantages: (1) It has a larger specific surface area, higher reactivity, and better repeatability, which make them more favorable to achieve higher sensitivity in clinical diagnosis [8, 9]. (2) It is label-free and has the potential to develop into a point-of-care technology with microelectronics [10, 11] for different target analytes such as drug molecules [12–14], nucleic acids [15, 16], proteins [17, 18], or cells [19, 20].

However, the development of OTFT-based biosensors still faces numerous challenges. For one thing, the sensitivity is still limited to meet the requirements for low-abundance proteins. For another, the determination in complex media might be disturbed easily by false-positive signals, which are not clinically accurate in early diagnosis. Therefore, effective functionalization strategies are essential to improve performance. Herein, recent developments of OTFT-based biosensors are presented for various life and health monitoring applications. Firstly, we introduced the composition and mechanism of OTFTs and related devices for sensing applications. Later, we exhibited several construction strategies, which mainly include: (1) design and synthesis of new materials; (2) modification or functionalization on sensing surface; and (3) integration with circuits and artificial intelligence. Afterwards, we described the approaches to achieve high-performance OTFT-based biosensors for life and health monitoring in both body fluids and exhaled gas. Finally, we discussed the perspectives of OTFT-based sensing technology in clinical diagnosis. This mini-review connects OTFTs with biomedicine to realize the construction of biological activity data, which provides a feasible new idea for the future digital, intelligent, integrated, and high-throughput detection of biomarkers.

2 Composition and mechanism of OTFT-based biosensors

Since the first OTFT was reported by Tsumura et al. [21] in 1986,

Address correspondence to Chenfang Sun, sunchenfang@email.tjut.edu.cn; Tie Wang, wangtie@email.tjut.edu.cn

OTFTs have received extensive attention in the following decades based on their unique characteristics of signal conversion and amplification for sensing applications. Compared with other technologies, OTFTs can directly identify biological signals and then quickly convert them into amplified and readable digital signals after integration with microelectronic systems for rapid and high-throughput screening in clinical diagnosis. Besides, organic semiconductor (OSC) materials not only have the advantages of easy chemical property regulation, lightweight, and comprehensive source, but also are suitable for low-temperature solution methods (spin-coating or ink-jet printing) with flexible substrates. Therefore, OTFTs are widely used in portable and label-free point-of-care biosensors with less sample volume, short analysis time, and wide linearity range.

Generally speaking, OTFTs are three-terminal electronic components with four device configurations: a gate electrode, a dielectric layer, source-drain electrodes, and an OSC layer [22] as shown in Figs. 1(a)–1(d). The charge carriers were injected from the source electrode to the conductive channel (several molecular layer thicknesses accumulation layer at the interface of OSCs with the insulating layer) under the regulation of the gate voltage (V_G). After that, the charge carriers moved directionally in the channel to generate the source-drain current (I_{SD}) with the regulation of the source-drain voltage (V_{SD}). The basic parameters used to evaluate the output performance of OTFTs include: (1) mobility (μ), the rate of charge carrier migration; (2) on/off ratio (I_{ON}/I_{OFF}), the ratio of I_{SD} from on-state to off-state; (3) threshold voltage (V_{TH}), the minimum V_G to turn on the OTFTs; and (4) subthreshold slope (SS), the speed of the OTFTs from off-state to on-state. The above basic parameters can be obtained by testing the transfer and output curves. The transfer curve is used to evaluate the variation of I_{SD} with V_G at constant V_{SD}, and the output curve is used to assess the variation of I_{SD} with V_{SD} at different V_G. When OTFTs are placed in an environment with a target analyte, the specific recognition between the analyte and the device causes a change in charge carrier concentration, which influences the transport characteristics of OTFTs.

Up to now, biosensors based on OTFTs can be classified into three categories according to different principles: (1) organic field-effect transistor (OFET)-based biosensors with a classical solid-state dielectric layer [23], where a field-effect mechanism generates the modulation of the electrical signal; (2) electrolyte-gate OFET (EGOFET)-based biosensors [24, 25], which are mainly based on the bilayer modulation between the gate/electrolyte and the OSCs/electrolyte; and (3) organic electrochemical transistor (OECT)-based biosensors [3, 26], which are mainly based on the doping/de-doping of ions in the OSCs. The device structures for OFET-based biosensors, EGOFET-based biosensors, and OECT-based biosensors are shown in Figs. 1(e)–1(g), respectively. Among them, OFET-based biosensors are usually applied for gas determination, while EGOFET-based and OECT-based biosensors are used in body fluids.

It is worth noting that OTFT-based biosensors' mechanisms differed between body fluids and exhaled gas in life and health monitoring. (1) In body fluids: The changes in output signals are related to the isoelectric point (pI) of charged molecules and the pH of the solution. Taking protein biomarkers as an example, when the pI is lower than pH value, a highly negative charge appears in the antibody-antigen complex. Compared with the baseline, the weak electrostatic interactions between the channel region and surface charges will induce a negative V_{TH} electrical signal shift. (2) In exhaled gas: The changes in output signals are related to the redox properties of gas molecules. For example, if the oxidizing gas (NO_2, O_2, and CO_2) is used as an electron acceptor, the hole carrier density and conductivity would increase,

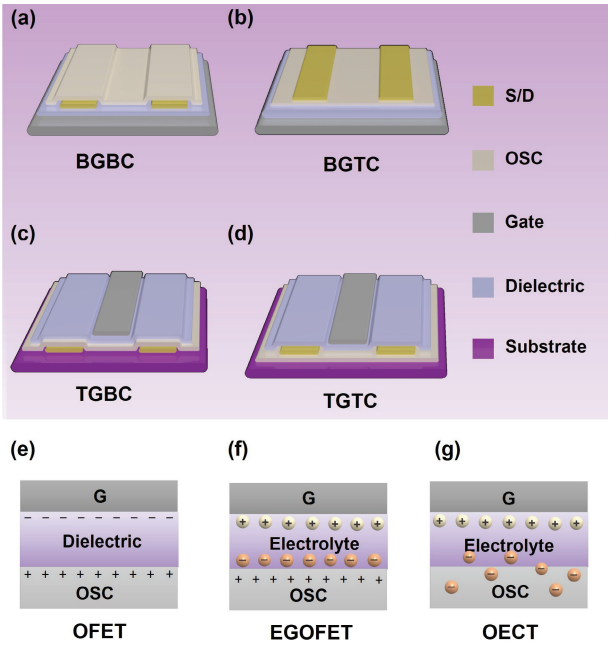

Figure 1 (a) The bottom-gate and bottom-contact (BGBC) structure of OTFTs. (b) The bottom-gate and top-contact (BGTC) structure of OTFTs. (c) The top-gate and bottom-contact (TGBC) structure of OTFTs. (d) The top-gate and top-contact (TGTC) structure of OTFTs. The transmission principles of (e) OFET, (f) EGOFET, and (g) OECT.

which induces an enhanced I_{SD} electrical signal compared with the baseline. Otherwise, reducing gas (H_2, H_2S, and CO) as an electron donor will reduce the hole carrier density and conductivity, thus decreasing I_{SD} electrical signal.

3 Construction strategies for OTFT-based biosensors

The keys to high-performance OTFT-based biosensors are the highly efficient transportation of charge carriers and efficient immobilization of sensitive probes, both of which are indispensable. Therefore, the sensing surface usually needs to meet the following requirements: (1) ensuring efficient immobilization of sufficient sensitive probes; (2) maintaining the activity of original sensitive probes; and (3) reducing the non-specific adsorption of the sensitive probes. Up to now, several optimized strategies exist for constructing OTFT-based biosensors.

3.1 Novel materials for OTFT-based biosensor

Due to the physicochemical properties of the target analytes to be tested, designing new materials with specific functional groups has received wide attention in sensing applications. The proposed new materials will reduce the energy of the response and make the reaction process faster, thus enhancing the interactions between target analytes and the devices and improving the sensing performance. Modifying molecular structure is a more direct and effective strategy to enhance the performance of OSCs. Katz et al. [27] introduced hydroxyl groups into the molecular terminal of 5,5'-bis(4-n-hexyl-phenyl)-2,2'-bithiophene (6PTTP6) to synthesize 5,5'-bis(4-hydroxyhexyloxyphenyl)-2,2'-bithiophene (HO6OPT) in Figs. 2(a) and 2(b). The results showed that the OH groups in HO6OPT can form hydrogen bonds with the dimethyl methyl phosphonate (DMMP), leading to increased adsorption and electronic effects. Therefore, the sensitivity was significantly improved with HO6OPT as the upper layer.

Afterwards, Huang et al. [28] explored the impact of the alkyl side chain of OSCs in NH_3 sensing. The authors reported four different alkyl side chain lengths with the same π-conjugated core

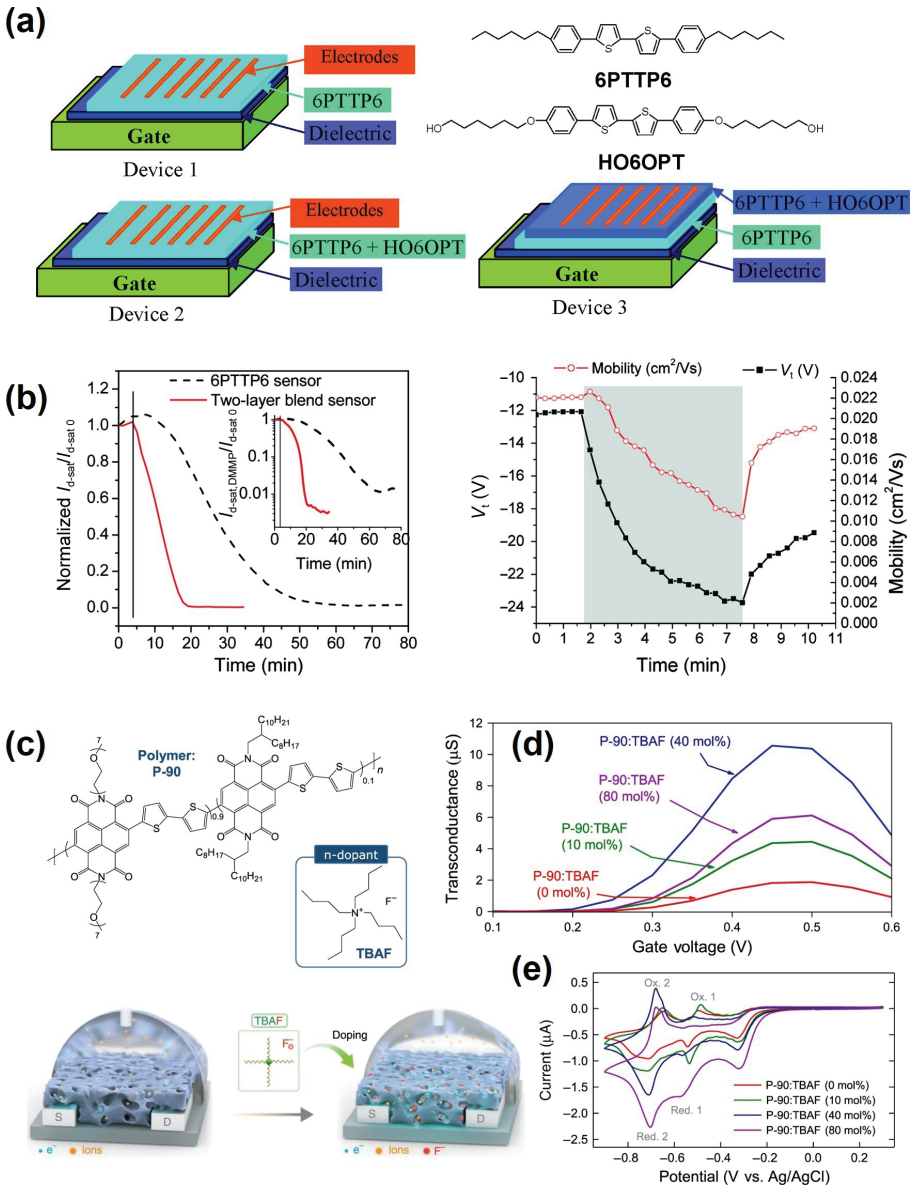

Figure 2 (a) Illustrations of OFETs and semiconductor molecular structures: 6PTTP6, single-layer blend, and two-layer blend. (b) Sensing responses to DMMP vapor (left, the inset shows the logarithmic plots of the same curves) and the changes of mobility and threshold voltage (right). Reproduced with permission from Ref. [27], © American Chemical Society 2007. (c) The structures of TBAF and P-90 and the device configuration with a graphical illustration of TBAF doping mechanism in P-90. (d) The transconductance results of P-90 containing 0 mol%, 10 mol%, 40 mol%, and 80 mol% TBAF. (e) Cyclic voltammetry measurements of P-90 containing 0 mol%, 10 mol%, 40 mol%, and 80 mol% TBAF. Reproduced with permission from Ref. [30], © Paterson, A. F. et al. 2020.

structure, and the results showed that the normalized responses to 1 ppm NH_3 were 4%, 24%, 33%, and 46% of 5,5'-bis(4-dodecylphenyl)-2,2'-bithiophene (12PTTP12), 6PTTP6, 5,5'-bis(4-ethylphenyl)-2,2'-bithiophene (2PTTP2), and 5,5'-diphenyl-2,2'-bithiophene (PTTP), respectively. The reasons could be concluded that the long alkyl side chain will hinder the diffusion of NH_3 into the OSCs, thus affecting the interaction between the target analyte and conducting channel. Besides, due to the intrinsic property defects of some materials, the sensing performance was not ideal when the material was applied as the active layer. In this case, additives can be inserted by doping or blending to synthesize novel composite materials for the target analytes. Xu et al. [29] demonstrated a skin-like finger-wearable driver for biomedical applications by blending poly(2,5-bis(2-octyldodecyl)-3,6-di(thiophen-2-yl)diketopyrrolo[3,4-c]pyrrole1,4-dione-alt-thieno[3,2-b]thiophen) (DPPT-TT) with polystyrene-block-poly(ethylene-ranbutylene)-block-polystyrene (SEBS) as the active layer with enhanced mechanical stretchability and high mobility of polymer OSCs. The author hypothesized that the nanoconfinement effect of DPPT-TT was achieved by forming the nanofibrils into a soft deformable elastomer, where excellent charge transfer was obtained through the connectivity between the nanofibril aggregates. In addition, Paterson et al. [30] demonstrated a novel strategy for stable OECTs through admixed tetra-n-butylammonium fluoride (TBAF) as a molecular dopant with polymer poly(N,N'-bis(7-glycol)-naphthalene-1,4,5,8-bis(dicarboximide)-co-2,2'-bithiophene-co-N,N'-bis(2-octyldodecyl)-naphthalene-1,4,5,8-bis(dicarboximide)) (P-90) in Figs. 2(c)–2(e), and the 40 mol% TBAF produced the best performance.

3.2 Surface modification for OTFT-based biosensor

Except for the properties of the materials mentioned above, the device surface modification attracted significant attention in the OTFT-based biosensor array. Generally speaking, the multielement biosensor array consists of various sensing materials. Thus, how to efficiently combine the sensing materials with the devices has been a broad concern in recent years.

Sharma et al. [31] summarized a series of synthetic receptors on

the surface to fabricate highly selective OTFT-based biosensors in Fig. 3(a). Briefly, the authors mentioned that the molecularly imprinted polymer (MIP) [32] is a widely used synthetic receptor due to its specific cavities for intermolecular recognition through ion–ion interactions, ion–dipole interactions, hydrogen bonding interactions, hydrophobic interactions, and van der Waals interactions. Recently, Minami et al. [33] functionalized OTFTs with MIPs as artificial receptors for the selective and sensitive capture of taurine. The results showed that the transfer curve was negatively shifted by adding taurine. The determination could be repeated at least five times, suggesting a more comprehensive health application in our daily lives. Besides, Wei et al. [34] demonstrated a transistor assay with multi-antibodies (CR3022, n3021, and S1) for highly sensitive and precise testing of antigens with different configurations in Figs. 3(b) and 3(c), including the "receptor binding domain (RBD) up", "one RBD down", and "two RBD down", respectively. The results illustrated that the multi-antibodies could bind not only the RBD but also the spike protein with different configurations, therefore improving the recognition efficiency of SARS-CoV-2 at 100% in 38.9 s. Besides surface modification, the functionalization of interfaces also received significant consideration in OTFT-based biosensors [35–37].

Besides, interface engineering is another crucial strategy for biosensors toward practical applications. There are four primary contact interfaces of OTFTs in Fig. 4(a), including electrode/OSC, dielectric/OSC, environment/OSC, and OSC/OSC interfaces, respectively. (1) Electrode/OSC interface: Tang et al. [38] paired pentafluorobenzenethiol self-assembled monolayers on source/drain electrodes to tune the charge-injection barrier and avoid the high contact resistance (R_q) while maintaining the morphology and performance of OSCs. Furthermore, to obtain linearly injected charge carriers, they released the strain by a one-step peeling strategy, which reduced π–π stacking distance and suppressed the generation of oxygen-doped carriers, eventually realizing an ideal OTFT in Fig. 4(b). (2) Dielectric/OSC interface: This interface is essential for efficient carrier transport. Therefore, modification of the dielectric layer by octadecyl trichlorosilane or inserting functional layers into the interface is another approach for improving sensor performance. Zhang et al. [39] combined an interlayer (IL) with high ionization energy into amorphous OSCs in Fig. 4(c), demonstrating that inserting a tris(4-carbazoyl-9-ylphenyl)amine (TCTA) IL provided an efficient injection of hole charge carriers from MoO_3 into the active film. (3) OSC/OSC

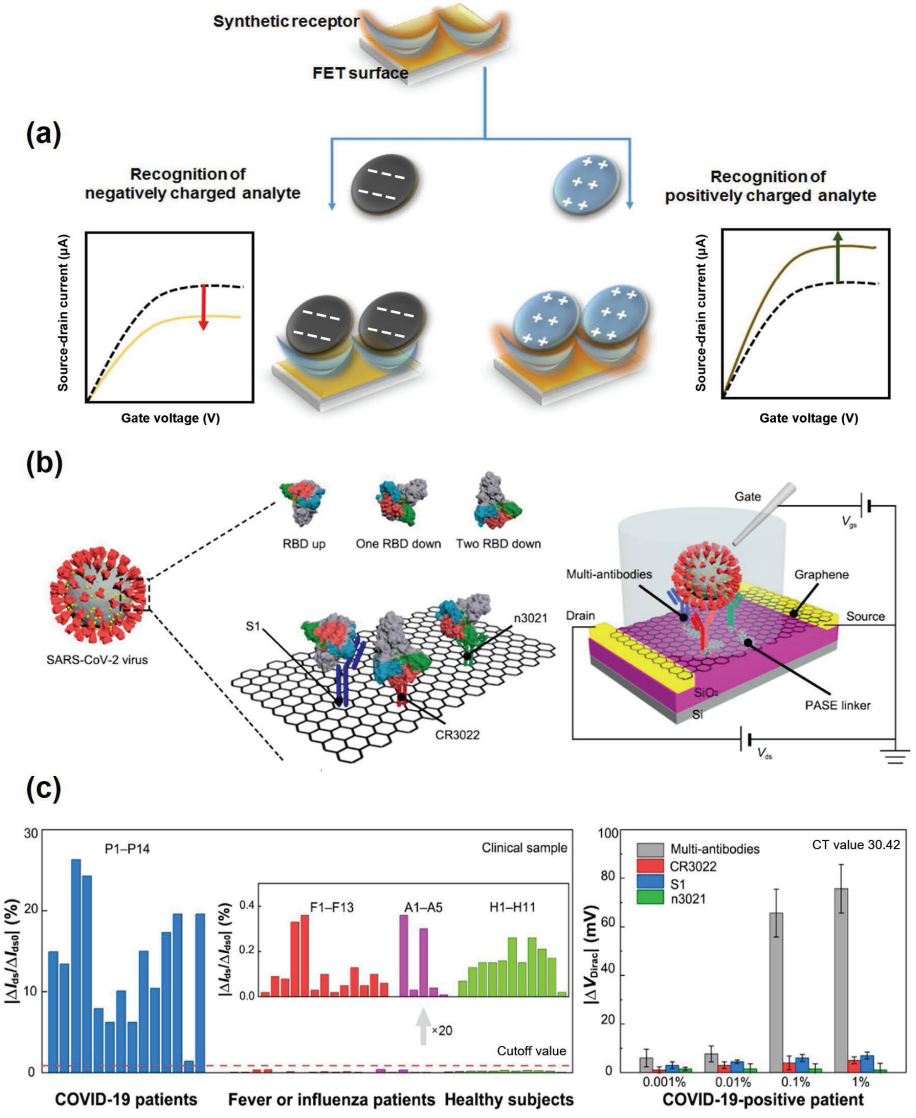

Figure 3 (a) Illustration of the transducer integrated with synthetic receptors, and recognitions of negatively charged analytes with decreased I_{SD} (left) and positively charged analytes with increased I_{SD} (right). Reproduced with permission from Ref. [31], © Elsevier B.V. 2018. (b) The binding events of SARS-CoV-2 on the surface with a 1-pyrenebutyric acid N-hydroxysuccinimide ester (PASE) linker. (c) The responses upon the addition of P1–P14, F1–F13, A1–A5, and H1–H11 on the left, and the comparison in the detection of the diluted clinical sample using multi-antibodies and single antibodies. Reproduced with permission from Ref. [34], © American Chemical Society 2021.

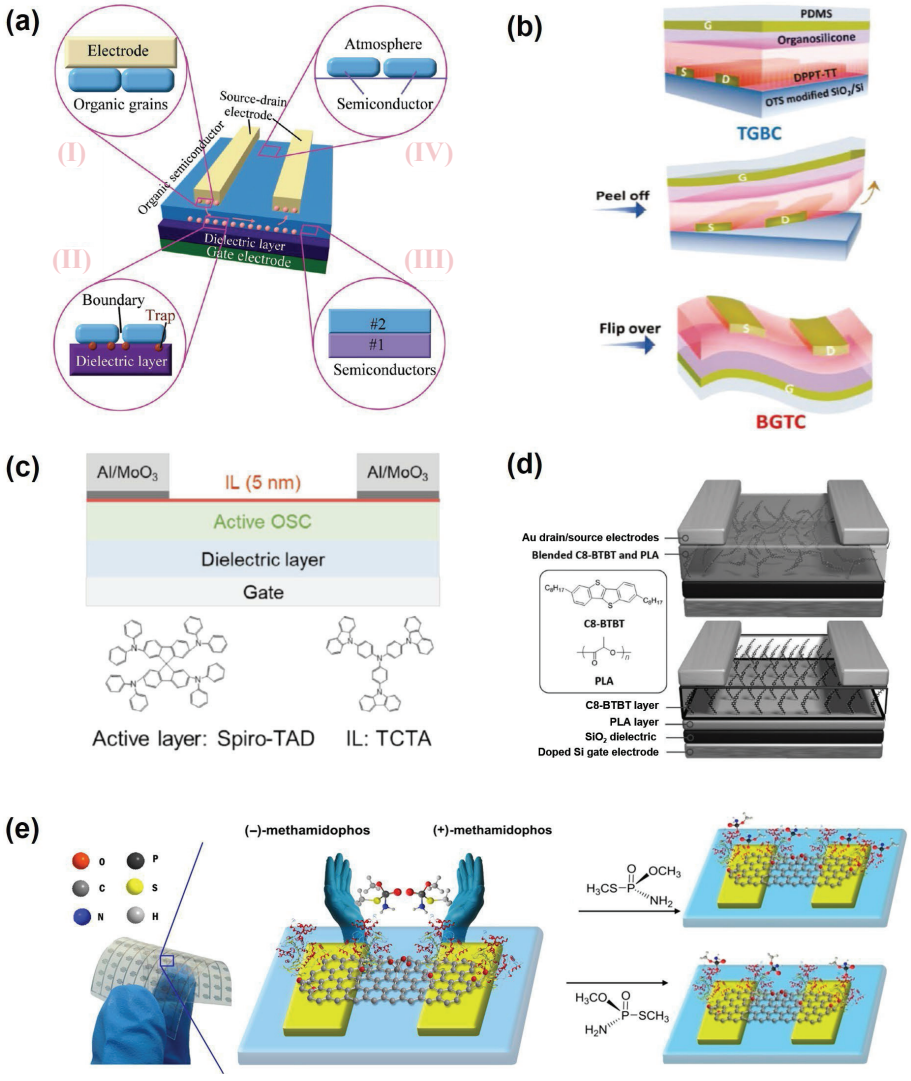

Figure 4 (a) Illustration of four primary interfaces in OTFT-based biosensors: (I) the interface of electrode/OSC layer, (II) the interface of dielectric/OSC layer, (III) the interface of OSC/OSC layer, and (IV) the interface of atmosphere/OSC layer. Reproduced with permission from Ref. [35], © American Chemical Society 2009. (b) Illustration of the one-step peeling strategy. Reproduced with permission from Ref. [38], © Wiley-VCH GmbH 2021. (c) The configuration of the BGTC transistor and the molecular structures of Spiro-TAD and TCTA. Reproduced with permission from Ref. [39], © Zhang, k. et al. 2020. (d) Chemical structures of C8-BTBT and PLA, and schematic diagrams of blended-device and layered-device. Reproduced with permission from Ref. [40], © WILEY-VCH Verlag GmbH & Co. KGaA, Weinheim 2017. (e) Illustration of reduced graphene oxide sensor modified with AChE for identifying enantiomers. Reproduced with permission from [41], © American Chemical Society 2019.

interface: Numerous kinds of researches have been reported for achieving high-quality thin films with excellent crystallinity and morphology through doping and blending strategies. Huang et al. [40] developed a high-performance, printable, and flexible OTFT by combining 2,7-dioctyl[1]benzothieno[3,2-b][1]benzothiophene (C8-BTBT) with polylactide (PLA) in Fig. 4(d). The improvements were attributed to a larger interfacial area between OSCs and polymers. (4) Environment/OSC interface: The OSC film is directly exposed to the target analytes in the environment. Thus, interface functionalization is essential for fabricating high-performance sensors. Liu et al. [41] modified acetylcholinesterase (AChE) as the recognition element in the sensing area (Fig. 4(e)). After the enantiomer was transferred to graphene, the sensors could achieve excellent discrimination of chiral molecules.

3.3 Integration OTFT-based biosensors with circuits and artificial intelligence

Based on the mentioned above, several types of researches have been devoted to developing bioanalytical systems, such as "lab-on-a-chip" based on OTFTs sensing arrays. With highly-crossed chemical and biological reactions on the sensing units of OTFTs, the detection of various target analytes could be achieved through multi-channel electrical signals. One of the critical steps in commercializing an OTFT-based sensing array is to fabricate large-area OSCs with homogeneous properties. Duan et al. [42] reported a large-area and highly-aligned organic crystalline array through a facile solution shearing technique to control the crystallographic orientation, crystal uniformity, and thickness. The results exhibited that the proposed array with good performance and uniformity can be applied to various sensing applications. With the rapid development of the Internet of Things (IoT), flexible wearable sensor devices are developing from proof-of-concept to practical applications. Liu et al. [43] demonstrated high-performance OTFTs with an ultrathin thickness of 380 nm by a simple spin-coating method, which have good conformability and can be adhered to human skin and used in wearable devices for health monitoring.

Nevertheless, there are still many challenges to realizing high-performance and reliability in OTFT-based biosensors. Yuan et al. [44] reported a clinically integrated urinalysis device array through interface engineering in Fig. 5(a) for directly simultaneous and reliable monitoring of five biomarkers associated with bladder

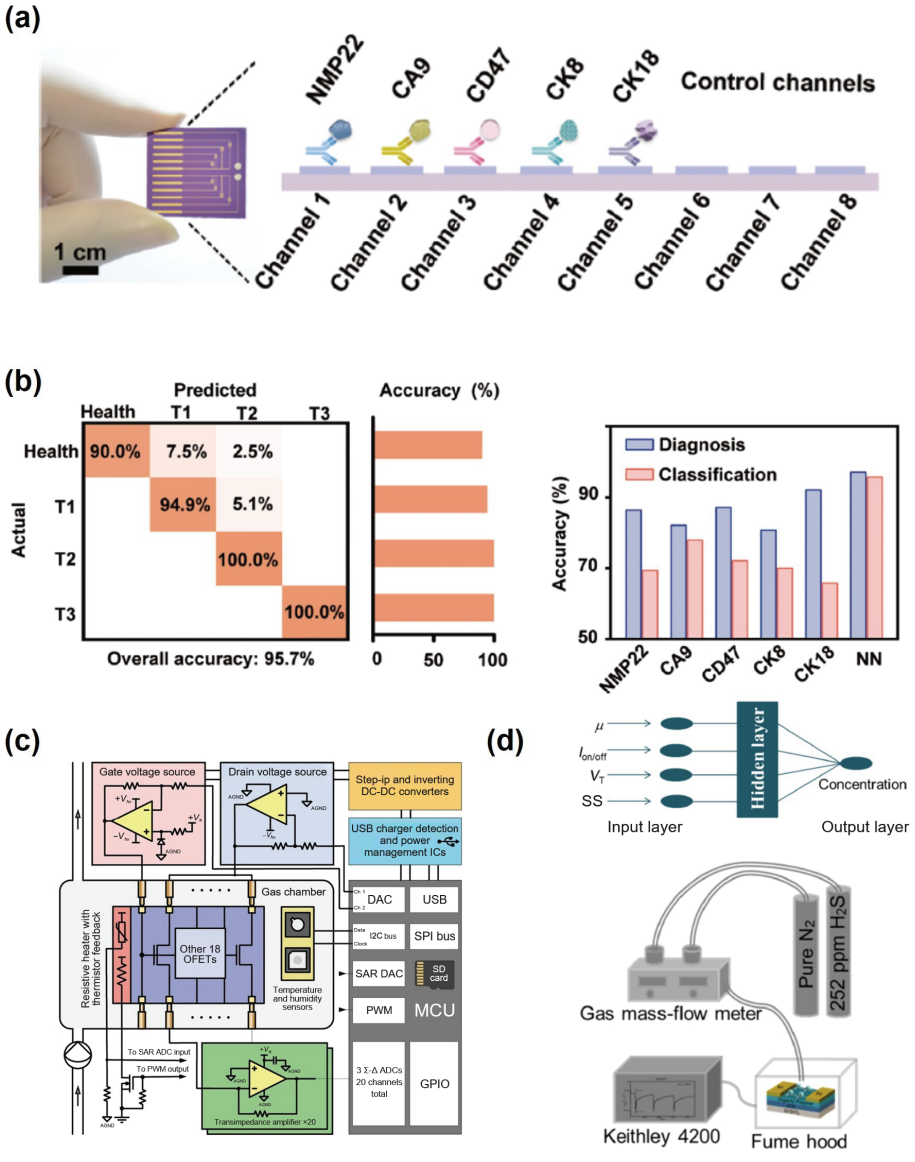

Figure 5 (a) Illustration of antibody-functionalized sensing array for bladder cancer. (b) Illustrations of the confusion matrix summarizing the classification for bladder cancer (left) and discrimination of patients from healthy individuals based on the neural network (NN) algorithm (right). Reproduced with permission from Ref. [44], © Wiley-VCH GmbH 2022. (c) Illustration of the whole array used to obtain all the data. Reproduced with permission from Ref [45], © Anisimov, D. S. et al. 2021. (d) Illustration of the test system based on OTFT for H_2S detection. Reproduced with permission from Ref. [46], © Elsevier B.V. 2022.

cancer. In addition, combined with a machine-learning algorithm in Fig. 5(b), the device can identify bladder cancer with an accuracy of 95% in a complex urine environment.

Besides liquid determination, the artificial olfactory system, such as the electronic nose, is the most mysterious hot topic for many scientists. Generally speaking, the electronic nose usually refers to a multi-sensor array that can specifically recognize complex odors by an appropriate recognition system and then transmit the obtained information to the recognition system. It has been rapidly developed in gas sensing based on the inherent advantages of OTFTs, such as diversity of molecular design, compatibility with solution process, and multi-parameter output characteristics. It has become a new gas-sensing technology for the specific recognition and identification of target analytes. Among them, miniaturization and intelligence are essential directions for developing high-performance gas sensors. Ponomarenko et al. [45] developed a fully integrated OTFT-based electronic nose in Fig. 5(c) for discriminating toxic air pollutants in noninvasive healthcare monitoring. The ultrasensitive OTFT-based sensor array was modified with different receptors on the OSCs to induce cross-selectivity. To further improve the accuracy, Wang et al. [46] combined an artificial neural network (ANN) with OTFT-based sensors in Fig. 5(d) for precise quantification and recognition of H_2S in 10 s with high responsivity (6500%) at 150 ppm.

4 Key requirements of OTFT-based biosensors for health monitoring

The so-called "biosensor" needs to integrate OTFTs and related devices with a digital signal readout system, such as a smartphone, to display the output signal in digital form. However, interference from non-specific adsorption is inevitable during practical applications in disease diagnosis. Thus, the performance of the biosensor assay needs to be further improved while ensuring sensitivity, selectivity, and stability.

4.1 The sensitivity (*S*) in OTFT-based biosensors

Sensitivity is the amount of signal change produced by the stimulus of the target analyte, which is usually expressed as a percentage of the change in output current to the initial current ratio $S = (I_S–I_0)/I_0 \times 100\%$, where I_S is the output current after exposure to the target analyte and I_0 is the initial current before the reaction of the target analyte. The limit of detection (LOD) is

usually used to guarantee the sensitivity and expressed as LOD = 3ε/k, where ε is the standard deviation and k is the slope of the calibration curve. However, the sensitivity is limited by the diffusion of analyte through the bulk films, thus remaining a significant challenge in the sensing field. Two main modification methods for improving the sensitivity are: (1) introducing porous structures on the semiconductor surface and (2) modifying specific functional groups. Both of them only have one purpose: increasing the interaction between the target analytes with carriers in the conducting channel.

For instance, Huang et al. [47] modified polystyrene microspheres on a plasma-treated substrate by freeze-drying to construct porous structures. Then the authors removed the polystyrene microspheres with tape, leaving a microporous structure on the surface in Fig. 6(a). The authors compared the performance before and after the modification to demonstrate that the porous OSCs can improve the sensitivity. The results showed that the signal changes were significantly enhanced after the modification. Besides, modifying metal–organic framework (MOF) materials with specific functional groups can also construct porous structures to increase the interaction area for sensing. Yuvaraja et al. [48] realized an ultrasensitive OTFT-based sensor via a novel isostructural-fluorinated MOF, which was used as a specific pre-concentrator of NO_2 in Figs. 6(b) and 6(c). In addition to this, the authors also explored the mechanism. The results showed that the MOF-A has higher electron affinity than poly{3,6-dithiophen-2-yl-2,5-bis(2-decyltetradecyl)pyrrolo[3,4-c]pyrrole-1,4-dione-alt-thienylenevinylene-2,5-yl} (PDVT-10), so more electrons are attracted to the MOFs, leaving excess holes in PDVT-10 and thus indirectly doping the OSCs. Finally, specific hydrogen bonding interactions between the target analyte diffusing inside and the inner surface of MOFs are used to promote the sensitivity and selectivity of the OTFT-based sensor.

Moreover, constructing patterned sensor arrays and applying them to the corresponding target detection improves the sensitivity OTFT-based biosensors. The orderly arrangement of the active materials can enhance the chance of collision and adsorption between the gas molecules and the transducer, therefore improving the detection sensitivity. Liu et al. [49] patterned supramolecules to integrate vertical and horizontal diffusion pathways in Fig. 6(d), which is conducive to improving the sensitivity of more than one order of magnitude than traditional sensors in detecting organic volatile compounds (VOCs).

4.2 The selectivity in OTFT-based biosensors

Selectivity, also known as cross-sensitivity, is the ability to accurately identify the target analyte in a hybrid system, such as serum, sweat, saliva, tears, urine, etc. However, the non-specific interactions between target analytes and OSCs lead to reduced

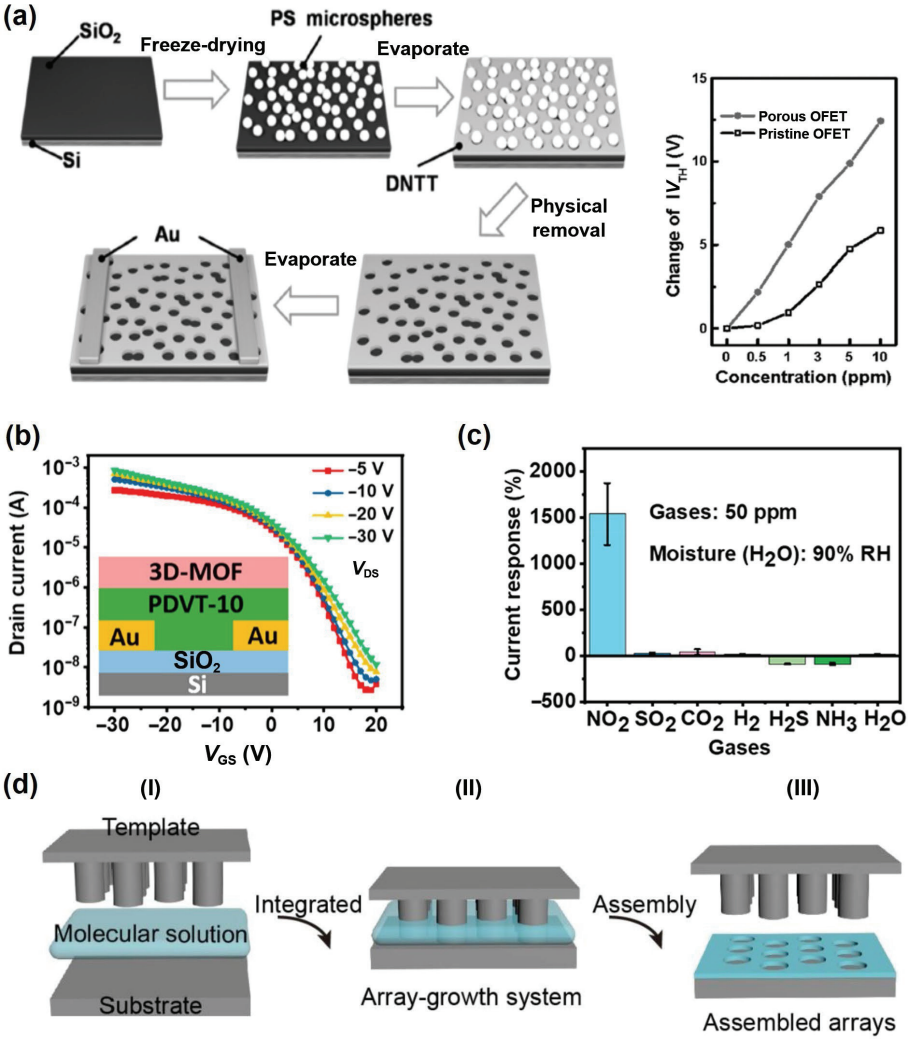

Figure 6 (a) The fabrication process of porous sensors (left) and the changes of $|V_{TH}|$ upon exposure to NH_3 (right). Reproduced with permission from Ref. [47], © WILEY-VCH Verlag GmbH & Co. KGaA, Weinheim 2017. (b) Transfer curves of the device with architecture at the inset. (c) Selectivity of the device for NO_2 determination. Reproduced with permission from Ref. [48], © American Chemical Society 2020. (d) The growth and patterning process for supramolecules by surface-structured templates. Reproduced with permission from Ref. [49], © Wiley-VCH Verlag GmbH & Co. KGaA, Weinheim 2020.

selectivity in most biosensors. Therefore, immobilizing sensitive probes, such as antibodies, enzymes, aptamers, and artificial protein receptors, is the most effective strategy to improve the specific recognition of target analytes. Several assembly strategies for immobilizing sensitive probes on sensing surfaces are split into noncovalent and covalent interactions. Noncovalent interactions can immobilize sensitive probes through intermolecular forces, such as van der Waals, hydrogen bonds, hydrophobic forces, ionic interactions, etc. In contrast, covalent interactions can form strong and irreversible chemical bonds by introducing functional groups (–CHO, –COOH, $–NH_2$, and –OH) that can covalently interact with sensitive probes on the surface.

For instance, the direct adsorption method is an immobilization technique that uses noncovalent interactions to adsorb sensitive probes directly onto the sensing surface, which is easy to operate and can effectively shorten the analysis time and reduce the preparation cost. Torsi et al. [50] constructed label-free EGOFET-based biosensors by immobilizing antibodies specific to procalcitonin (PCT) as a sensitive probe by direct adsorption. The entire preparation and detection processes were rapid, enabling the detection of PCT within 45 min at LOD = 2.2 pM (Figs. 7(a) and 7(b)). Besides, molecular self-assembly is a method to immobilize sensitive probes through chemical bonding efficiently. There are two types of self-assembling monolayer (SAM) systems: (1) SAM system formed on silicon or metal oxide surface by silylation reaction. 3-Aminopropyltriethoxysilane was modified on α-sexithiophene (α6T) films to form SAMs as immobilization sites by silylation reaction (Fig. 7(c)), enabling the biosensor to specifically detect penicillin in the micrometre range [51]. (2) SAM system formed on the gold surface by Au–S chemical bonding. Minamiki et al. [52] achieved specific detection of histidine-rich bovine serum by modifying the artificial protein receptor Ni^{II}-nitrilotriacetic acid (Ni^{II}-nta) on the electrode surface using Au–S chemical bonding (Fig. 7(d)).

Moreover, Kim et al. [53] immobilized monoclonal antibodies to the prostate antigen on the surface of gold nanoparticles (AuNPs) by Au–S chemical bonding, significantly improving the sensitivity and expanding the detection range. In addition, tailoring the molecular structure of OSCs through a covalent cross-linking method is a vital strategy to achieve efficient immobilization of sensitive probes for better sensing performance. Recently, Shen et al. [54] introduced carboxylic acid functional groups as molecular antennas on the sensing surface of OTFTs by plasma-assisted interfacial grafting method, enabling ultra-sensitive detection of adenosine triphosphate with a detection limit of 0.1 nM.

4.3 The stability in OTFT-based biosensors

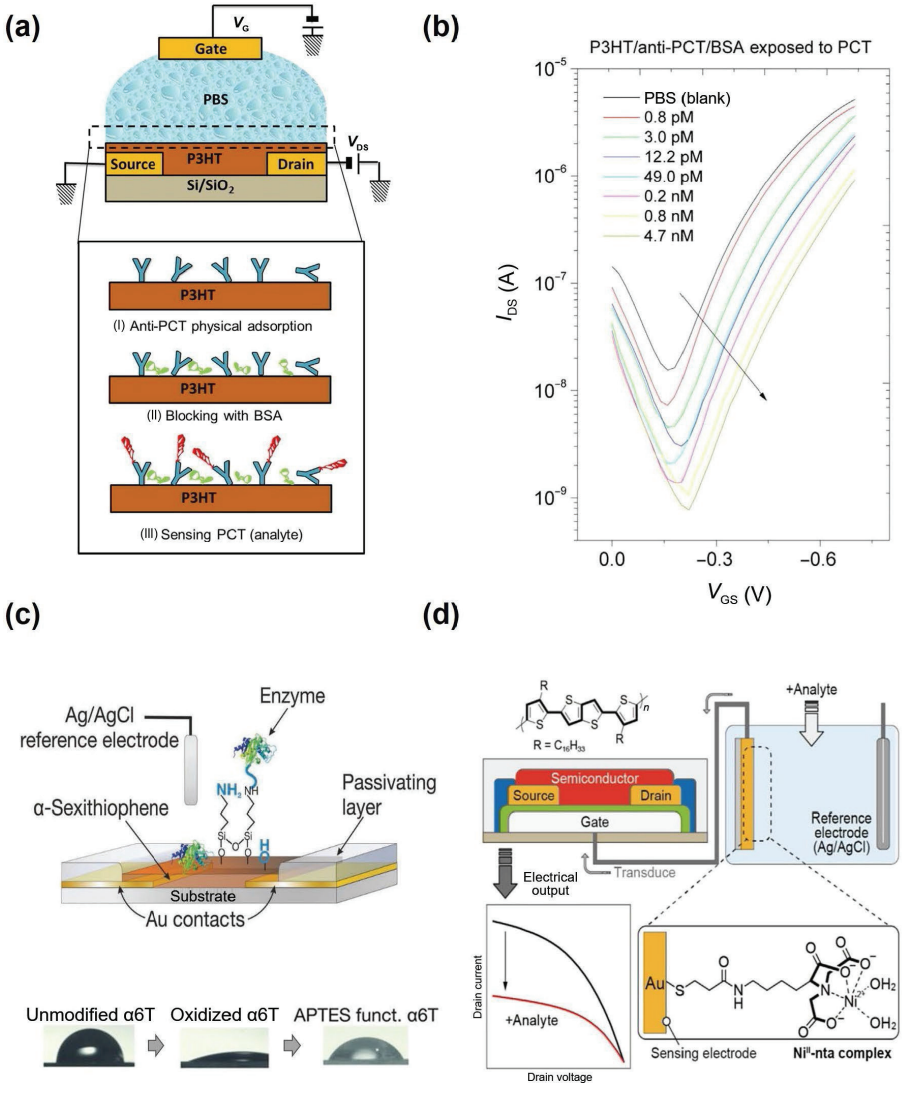

Figure 7 (a) Illustration of the EGOFET-based biosensor for PCT detection. (b) The transfer curves of P3HT/anti-PCT/bovine serum albumin (BSA)-based sensor exposed to PCT with different concentrations. Reproduced with permission from Ref. [50], © Elsevier B.V. 2017. (c) The transistor with varying steps of functionalization and contact angle measurements of treated α-sexithiophene thin films. Reproduced with permission from Ref. [51], © WILEY-VCH Verlag GmbH & Co. KGaA, Weinheim 2012. (d) The electrode is functionalized with an Ni^{II}-nta monolayer. Reproduced with permission from Ref. [52], © Minamik, T. et al. 2017.

Stability, including operational and storage stabilities, refers to the ability to output a stable and repeatable signal during repeated operations and the degree of performance degradation after a prolonged storage period. The lower the degree of degradation, the better the storage stability of the device. In recent years, research on improving the stability of OTFT-based biosensor has attracted significant attention. Jurchescu et al. [55] first explored the primary sources of instability and then introduced a method to eliminate the instability of OTFTs through packaging. Specifically, the primary source of instability is carrier trapping, which might lead to a decrease in I_{SD}, a shift in V_{TH}, and an increase in SS, limiting the development of OTFTs in practical sensing applications. To avoid the adverse effects of instability, the authors introduced parylene N for encapsulation by reducing H_2O introduction and increasing O_2 penetration, significantly improving device stability in Figs. 8(a) and 8(b). To further explore the mechanisms, the authors proposed three chemical defects, O_H, H_i, and OH_i, responsible for the trap states. The results showed that the H_i defects are more likely for the observed hole traps, while O_H defects are not accountable for the traps. Therefore, it is necessary to shield H_2O but permeate O_2 into the OSC.

At the same time, to reduce the introduction of water, molecular additives can be added to replace the water in the voids of the polymer film. Sirringhaus et al. [56] proposed that adding 2 wt.% tetracyanoquinodimethane (TCNQ) in the polymer solution would obtain excellent stability. The reasons are that TCNQ additive may interact strongly with the residual water molecules in the void after a prolonged annealing period and replace the H_2O in direct contact with the polymer, thus improving the stability.

After that, Sirringhaus et al. [57] also proposed that a long annealing time is critical for higher bias stress stability. The

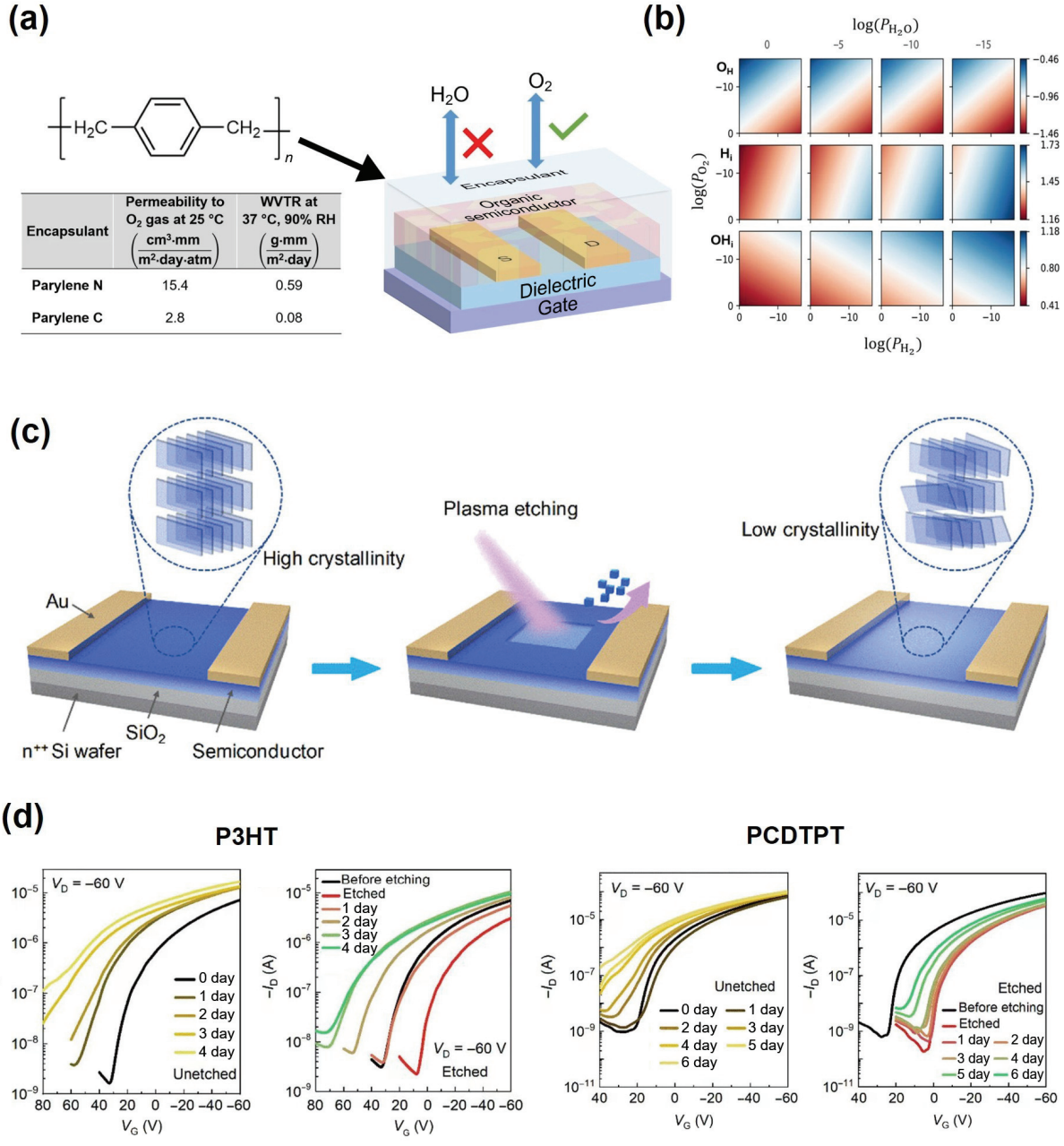

Figure 8 (a) The proposed device is encapsulated with parylene N, allowing O_2 while preventing the permeation of H_2O. (b) Chemical defect formation energy as a function of O_H, H_i, and OH_i. Reproduced with permission from Ref. [55], © Iqbal, H. F. et al. 2021. (c) The soft plasma etching by low-pressure plasma. (d) The performances of unetched and etched transistors for P3HT (left) and PCDTPT (right). Reproduced with permission from Ref. [59], © American Chemical Society 2021.

authors hypothesized that long-time annealing below the boiling point could allow the reorganization of polymer in the solvent, thus improving the bias stress stability. In addition, Kippelen et al. [58] utilized fluoropolymer CYTOP and Al_2O_3:HfO_2 as a double-gate dielectric layer to enhance stability. The second dielectric layer compensates for the shift of V_{TH} caused by the captured carriers, thus generating the opposite V_{TH} to the first dielectric layer over time, ultimately making the device more stable overall. Besides, to further explain the illustration, the authors proposed two compensating aging mechanisms: the single stretch exponent (SSE) model and the double stretch exponent (DSE) model. The results showed that the DSE model can be better fitted than the SSE model. In addition, the surface etching technique was also utilized to improve the environmental stability of OTFTs. Zhai et al. [59] performed a low-pressure plasma etching for the polymer film to remove the surface layer of the channel in Figs. 8(c) and 8(d), which is a non-destructive treatment for the transistors based on poly(3-hexylthiophene) (P3HT) and poly[4-(4,4-dihexadecyl-4H-cyclopenta[1,2-b:5,4b']dithiophen-2-yl)-alt[1,2,5]thiadiazolo[3,4-c]pyridine] (PCDTPT), respectively. Therefore the lifetime was increased by over 50%.

5 Detection of biomarkers in body fluids and exhaled gas

People's living quality and standards have been greatly improved due to the rapid development of society. However, along with these improvements in living standards, the probability of some diseases has increased owing to the unhealthy diets. It is worth mentioning that many diseases have no noticeable symptoms in their early stage, which significantly increases the incidence of illness and makes it difficult to cure. Detecting disease biomarkers, such as proteins, deoxyribonucleic acid, hormones, and metabolites in body fluid, can significantly improve the health of people's lives. In addition, some components of gas biomarkers in human exhaled breath, such as endogenous volatile markers, are also closely related to certain diseases and used as health warnings.

5.1 Determination of macromolecules in body fluid

In recent years, chemometrics work has become more apparent in people's life and health for early disease diagnosis. For instance, Cheng's group recently reported a series of high-performance biosensors for simultaneous biomarker determination [60–62]. The basic principles enhance the interactions between the analytes and OSCs by introducing functional groups, which results in carrier density changes, thus leading to the evolution of characteristics. In addition, the single-molecule transistor (SiMoT) platform based on OTFTs [63–65] has gradually developed for ultra-low-abundance biomarker determination in body fluid. The ultra-high sensitivity is up to the physical limit of fg level. Taking the coronavirus disease 2019 (COVID-19) as an example, Wei et al. [15, 16] first integrated a transistor into a "molecular electromechanical system" with long-term stability. When the electric field was applied, the flexible cantilever approached the device surface and induced noticeable changes in electrical signals. The whole process could be finished within 4 min, and the LOD was one to two copies in 100 μL.

Besides, Guo et al. [66] reported an SiMoT platform based on the nanobody-functionalized gate electrode, where the specific binding would cause the signal change, and finally achieving ultra-high sensitivity determination of SARS-CoV-2. To further investigate the mechanism, Macchia et al. [64] suggested the principle that the antigen-antibody binding event on the biological-SAM (Bio-SAM) layer triggers a tiny defective region in the chemical-SAM (Chem-SAM) (Figs. 9(a) and 9(b)), which starts an electrostatic hydrogen bonding network that causes changes in the power function, therefore affecting the difference in the output signals.

Nevertheless, the diffusion process of the target analyte from the solution to the biosensor surface may need several hours for biorecognition. Herein, Koklu et al. [67] integrated alternating current electrothermal (ACET) flow into an OECT-based sensor in Figs. 9(c) and 9(d) to accelerate the incubation and operation. The results showed that the recognition of the biomarker was in only 2 min with the LOD at 100×10^{-18} M. Except for the ACET technique, Yan et al. [68] also developed an ultrafast, label-free, and portable platform for SARS-CoV-2 detection based on voltage pulses to accelerate the specific detection. Recently, to solve the adverse effects of new coronavirus mutations, Zhang et al. [69] reported an inexpensive bioassay for the rapid colourimetric recognition of viral RNAs (SARS-CoV-2) within 30 min, and the sensing signals were obtained from the changes in pH via a smartphone.

5.2 Determination of small molecules in body fluid

Apart from protein biomarkers, the determination of small biological molecules such as genetic material [70–76], glucose [77–79], lactate [80, 81], dopamine [82–85], and cortisol [86–90] is of great importance for health monitoring. Among them, DNA has a double helix molecular structure and genetic information, and complementary base pairing can achieve the target analytes identification. Gao et al. [75] reported a field-effect transistor (FET) based on graphene to determine miRNA in Fig. 10(a), and the whole process of reaction and detection was finished in 20 min with the LOD of 10 fM. Besides, lactate is another critical indicator of diseases such as ischemia, infectious shock, liver disease, organ failure, and stroke. Thus, lactate detection has potential applications in clinical medicine. Chan et al. [77] modified the gate electrode for a compassionate determination of glucose and lactate in Fig. 10(b), which could be finished in 1 min with a low sample volume of 30 μL.

In addition, dopamine is a neurotransmitter in the blood of the human nervous system and is associated with many neurological disorders. Yan et al. [84] reported a novel transistor inherited the high porosity of Cu_3(2,3,6,7,10,11-hexahydroxytriphenylene)$_2$ (Cu_3(HHTP)$_2$), which maintained high sensitivity and exhibited excellent charge transportation properties, offering great applications in various aqueous environments. Moreover, the abnormal cortisol concentration in the body is closely related to physical and mental health. Khan et al. [88] improved sensitivity by modifying cortisol monoclonal antibody (c-Mab) at the gate electrode and generating photocurrent by laser irradiation in Fig. 10(c), resulting in a low detection limit of 1 pM for cortisol in human saliva samples. To further improve the sensitivity, a high-performance biosensor for cortisol detection in saliva was fabricated based on multi-dimensional carbon nanofiber (CNT) FETs, which has accurate selectivity, stable reusability, and high sensitivity for cortisol molecules [87]. Compared with the smooth surface, the needle-like structures of CNT film had a more available surface area for antibody immobilization, resulting in an extreme cortisol sensitivity of 100 aM.

5.3 Determination of biomarkers in exhaled gas

Since the first polythiophene-based OTFT was reported in 1986, it has attracted widespread attention in gas sensing [4]. It now plays an essential role in detecting gases, such as ammonia, nitrogen dioxide, hydrogen sulfide, and VOC. The mechanism can be expressed as follows: When the OTFT-based gas sensor is exposed to the target gas analyte, the noncovalent interactions [91] between OTFTs and the target analyte result in the change of carrier

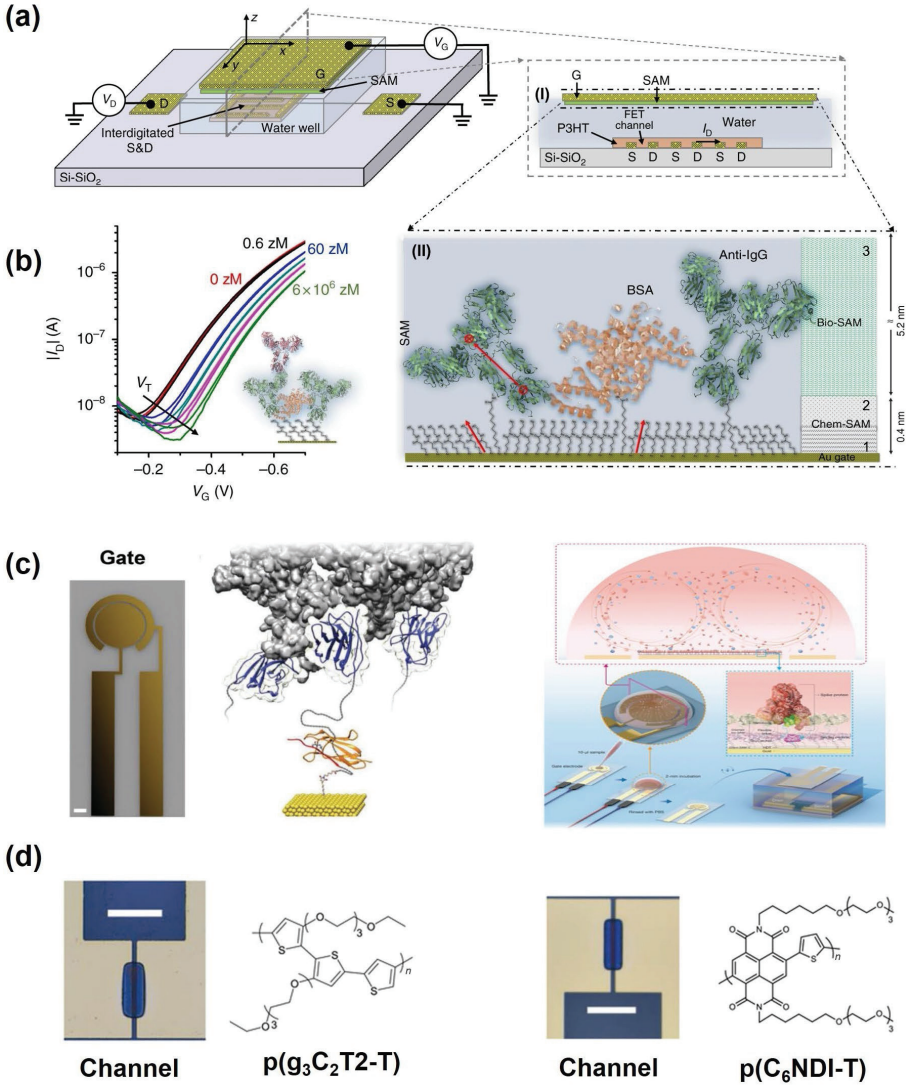

Figure 9 (a) The structure of SiMoT transistor based on OFET: (I) the cross-sectional structure of the transistor with source and drain electrodes, and (II) illustration of a functionalized gate electrode with Chem-SAM and Bio-SAM for capturing proteins. (b) Sensing measurements of the SiMoT exposed to immunoglobulin-G (IgG) at zM level. Reproduced with permission from Ref. [64], © Macchia, E. et al. 2018. (c) The gold gate electrode applied to the ACET flow (left) and an illustration of the ACET-enhanced nanobody-OECT biosensor (right). The scale bar is at 100 μm. (d) The ACET-enhanced nanobody-OECT biosensors with p-type p(g_3C_2T2-T) (left) and n-type p(C_6NDI-T) (right). Reproduced with permission from Ref. [67], © Wiley-VCH GmbH 2022.

transport properties, therefore leading to the variations in device characteristics. However, such reaction-assisted detection faces the challenges of low sensitivity and poor selectivity due to weak interactions, such as electrostatic interaction, weak van der Waals interaction, dipole interaction, and hydrogen bond interaction between the gas analyte and the OSC. There are several strategies for improving the performance of OTFT-based gas sensors.

(1) Modifying the surfaces between the OSC layers and the target gas molecules: Chi et al. [92] introduced different SAMs on the OSC surface to fabricate highly selective organic gas sensors in Fig. 11(a). In addition to modifying functional groups, a selective membrane also plays a vital role in improving the selectivity. Deng et al. [93] demonstrated a kind of OECT-based nitric oxide (NO) sensor with poly-5-amino-1-naphthol (5A1N) for achieving optimum signal amplification of target analytes with a lower detection limit, a more comprehensive linear range, a higher sensitivity, and a more excellent selectivity. (2) Optimizing the sensing layer thickness, morphology, and microstructure: Jiang et al. [94] reported an ultrasensitive OTFT-based gas sensor in Fig. 11(b) by exploiting monolayer molecular crystals (MMCs) with porous two-dimensional structures forming *in situ* for NH_3 determination at sub-ppb level. Besides, Huang et al. [47] demonstrated a porous OTFT-based ammonia sensor by a simple vacuum freeze-drying template method, and the results exhibited a much higher sensitivity (340% ppm^{-1}) than that of the pristine OTFTs when exposed to NH_3. (3) Integrating the receptor materials into OTFT-based sensors: Zhang et al. [95] reported a gas sensor by introducing tert-butoxy carboxyl groups into the side chains of diketopyrro-lopyrrole (DPP)-based conjugated polymer to synthesize pDPPBu-BT with remarkable high sensitivity and selectivity for the determination of ammonia and other amines. The proposed sensor could detect ammonia down to 10 ppb with negligible interference from other volatile analytes. Afterwards, Zhang et al. [96] also prepared PDPP4T-T by incorporating thymine groups into the DPP side chains (Fig. 11(c)), significantly improving the sensing performance of OTFT-based sensor. The results in Fig. 11(c) exhibited that the responses toward CO and H_2S were at 10 and 1 ppb after contained Pd(II) and Hg(II) ions into PDPP4T-T. Under this general environment, finding new gas-sensitive materials or using various doping and modification methods for current gas-sensitive materials are also highly important for developing high-performance sensors in the future.

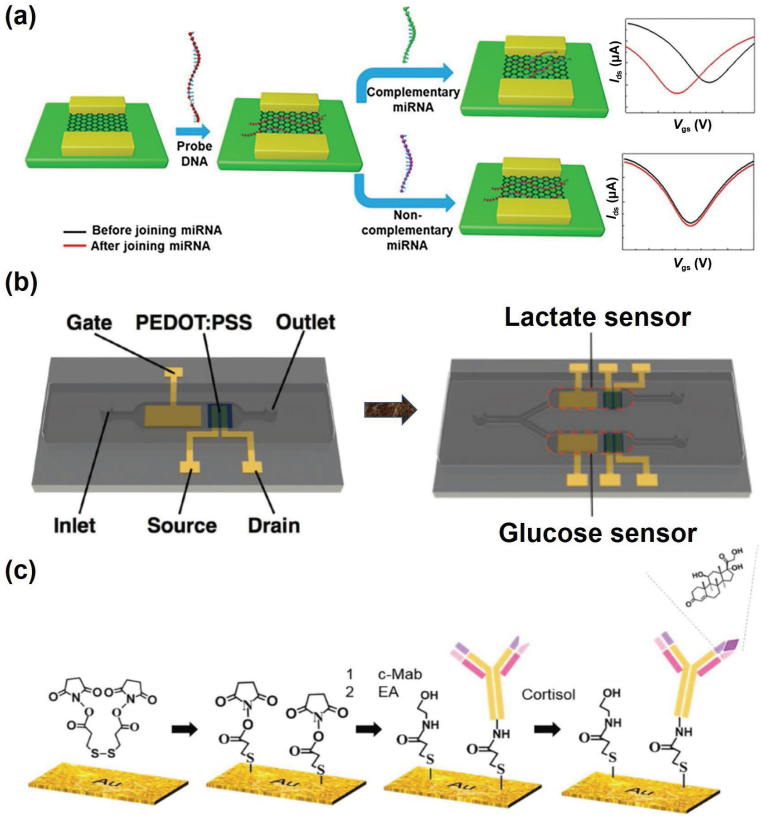

Figure 10 (a) Illustration of the biosensor for miRNA detection. Reproduced with permission from Ref. [75], © American Chemical Society 2020. (b) Illustration of OECT-based sensor for both glucose and lactate determinations. Reproduced with permission from Ref. [77], © WILEY-VCH Verlag GmbH & Co. KGaA, Weinheim 2016. (c) Illustration of chemical treatment for cortisol identification. Reproduced with permission from Ref. [88], © Elsevier B.V. 2020.

5.4 Overcoming the Debye and diffusion effects

The interface between the OTFT-based biosensor and target analyte strongly affects the device response. Thus, basic mechanisms should be understood for the binding of antibody-antigen, the hybridization of DNA and RNA, and the interactions of receptor ligands in the solution [97]. It is worth mentioning that the sensitive detection of biomolecules in body fluid will face significant challenges due to the limitation of the Debye length (λ_D), which causes a charge-shielding effect when the size of the target analyte exceeds the λ_D. Therefore it is difficult for OTFT-based biosensors to detect changes in the electrical signals. Taking phosphate buffer solution (PBS) as an example [98], the λ_D in 1 × PBS, 0.1 × PBS, and 0.01 × PBS are referred to as 0.7, 2.3, and 7.3 nm, respectively. To overcome the limitations of λ_D, bilayer phospholipids (PLs) were immobilized on the surface of OSCs (Fig. 12(a)) [99], and based on the high affinity of PL for streptavidin and avidin, the capacitive effect influences target identification by Donnan's equilibria [100] rather than electrostatically dominated, so the detection does not depend on the limitation of λ_D. Besides, Song et al. [101] constructed OTFT-based devices with an extended gate structure, which separated the sensing region and OSCs. Briefly, polyethene glycols (PEGs) of different molecular weights were modified on the extended electrodes to increase the λ_D, which led to a selective glial fibrillary acidic protein (GFAP) determination, showing excellent application prospects.

In addition to the problems encountered in liquid testing mentioned above, the efficient diffusion of gas molecules is another critical factor for improving the sensitivity. Chung et al. [102] designed a porous film by breath-figure (BF) molding of donor–acceptor copolymers OSCs, and the results exhibited that a high-performance OTFT-based gas sensor was fabricated with high responsivity (104%), excellent sensitivity (774% ppm^{-1}), and low LOD for NO_x (110 ppb) in 100–300 s at room temperature. To further understand the mechanism of efficient diffusion in Fig. 12(b), Qiao et al. [103] developed a kind of microarray sensor with a hollow nanocage on Ag nanowires to fabricate Ag@layered double hydroxide (LDH) by a templating route in Fig. 12(c), which exhibited a significant improvement in the ability of adsorbed and captured gas molecules compared with Ag nanowires and Ag@zeolitic imidazolate framework (ZIF)-67, demonstrating the practical potential for gas biomarker screening. After that, Xue et al. [104] fabricated an AuNPs-bridge array to increase the target analytes' collision probability and mass transfer efficiency. The results demonstrated that the bridge array exhibited a 15-fold higher sensitivity than the planar array. Finally, Zhao et al. [105] made full use of nanoparticles and reported a binary nanosphere array containing simultaneous collection, pre-separation, and determination of analytes, which enabled a new opportunity in health monitoring.

6 Biomimetic applications of OTFT-based biosensors

Over the last decades, the trace of OTFT-based biosensors developed from a single device (nonliving) to an integrated biosystem (living) for life and health monitoring. Just as the human body is composed of various organ systems, a series of techniques are constructed to make OTFTs more suitable for biomimetic applications, such as the visual, tactile, olfactory, and memory systems. This part summarizes the latest advances in OTFT-based biosensors for biomimetic systems, synapses, and neural networks. Firstly, developing biomimetic systems based on OTFTs, including the electronic eye, electronic nose, and electronic tongue, has attracted significant attention. Choi et al.

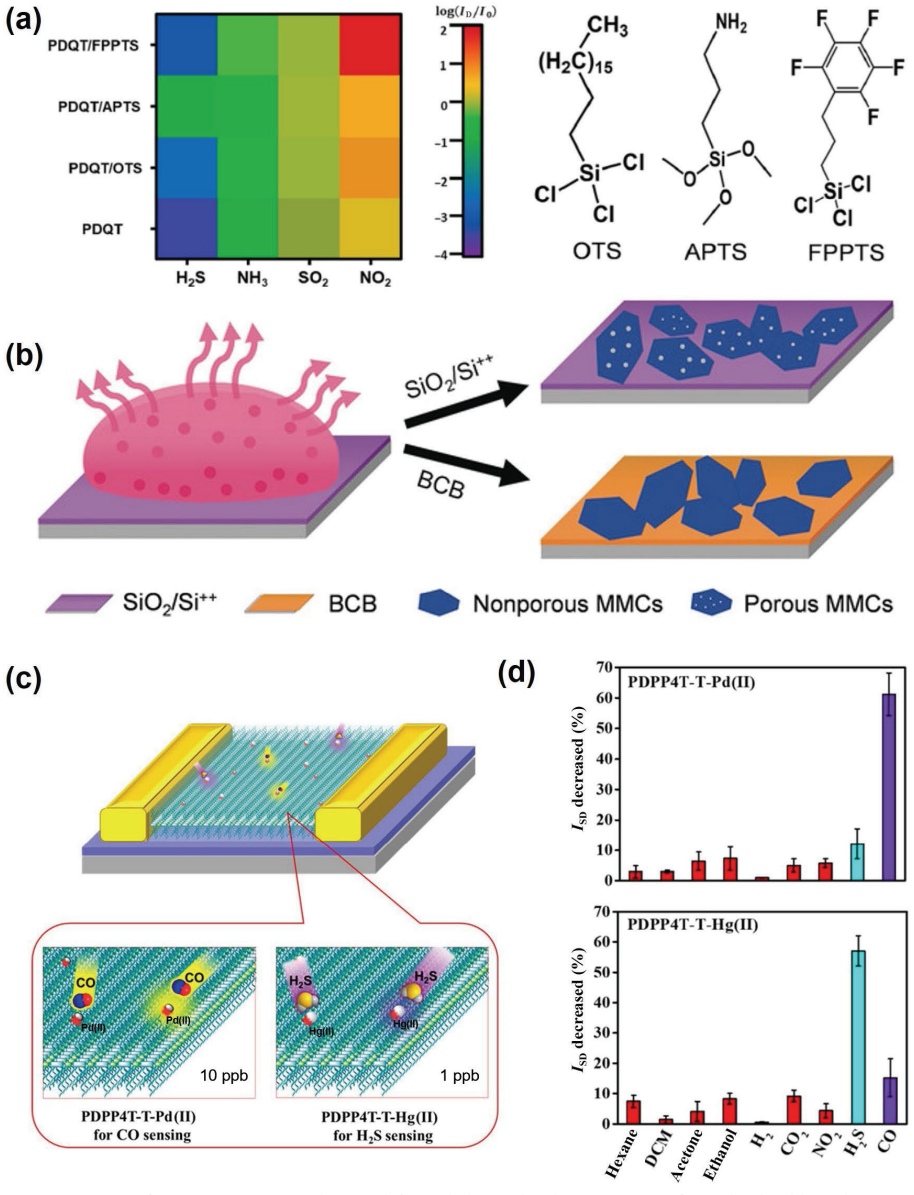

Figure 11 (a) The sensitivity variations of H_2S, NH_3, SO_2, and NO_2 (left) and the molecular structures of octadecyltrichlorosilane (OTS), 3-aminopropyltrimethoxysilane (APTS), and penta-fluorophenylpropyltrichlorosilane (FPPTS) (right). Reproduced with permission from Ref. [92], © Elsevier B.V. 2021. (b) Illustration of the MMCs. Reproduced with permission from Ref. [94], © Li, H. Y. et al. 2020. (c) The sensing performance of OTFT-based sensors toward CO and H_2S with the incorporation of Pd(II)/Hg(II). (d) The changes in I_{SD} after exposure to different gases. Reproduced with permission from Ref. [96], © American Chemical Society 2019.

[106] reported a curved neuromorphic image sensor array (cNISA) to emulate a human visual recognition system based on a heterostructure of MoS_2 and poly(1,3,5-trimethyl-1,3,5-trivinyl cyclotrisiloxane) (pV3D3) in Fig. 13(a). The proposed imaging system enables image acquisition and recognition through a single readout without complicated optical components, which promotes the development of the next generation of an electronic eye. To further simplify the construction process, Han et al. [107] demonstrated an electronic nose composed of an semiconductor metal oxide (SMO) gas sensor and an metal–oxide-semiconductor field-effect transistor (MOSFET)-based 1T-neuron to mimic a biological olfactory neuron in Fig. 13(b). Compared with the traditional electronic nose, the proposed device uses a spiking neural network (SNN) rather than the deep neural network (DNN), which demands an energy-efficient system getting rid of circuits, CPU, and memory for application in the IoT. Based on the MOSFET, the same group [108] demonstrated an electronic tongue using Al_2O_3 and sodium ionophore X as sensing materials to mimic a biological gustatory neuron with reduced energy consumption in Fig. 13(c). The proposed artificial gustatory neuron can detect ion concentrations (pH and sodium ion) on an extended gate and then encode spike signals on the MOSFET, which acts as an input neuron in an SNN. Besides, visual and tactile synapses based on OTFTs also attracted significant attention in artificial biomimetic applications. Li et al. [109] fabricated a stretchable MoS_2 FET on elastomeric polydimethylsiloxane (PDMS) substrates with stable performances (30 $cm^2/(V·s)$) for visual synapse in Figs. 14(a) and 14(b). The proposed device was also used to mimic paired-pulse facilitation, short-term/long-term memory, and long-term potentiation/depression successfully.

Moreover, according to the excellent biocompatibility, the device exhibits great potential for bioelectronics and neural network simulation with a high image recognition accuracy of 95%. For further imitating the complex biological neural networks, Mo et al. [110] built up an intelligent tactile recognition system based on a multi-terminal MoS_2 synaptic transistor in Figs. 14(c) and 14(d), which not only simulates various biological

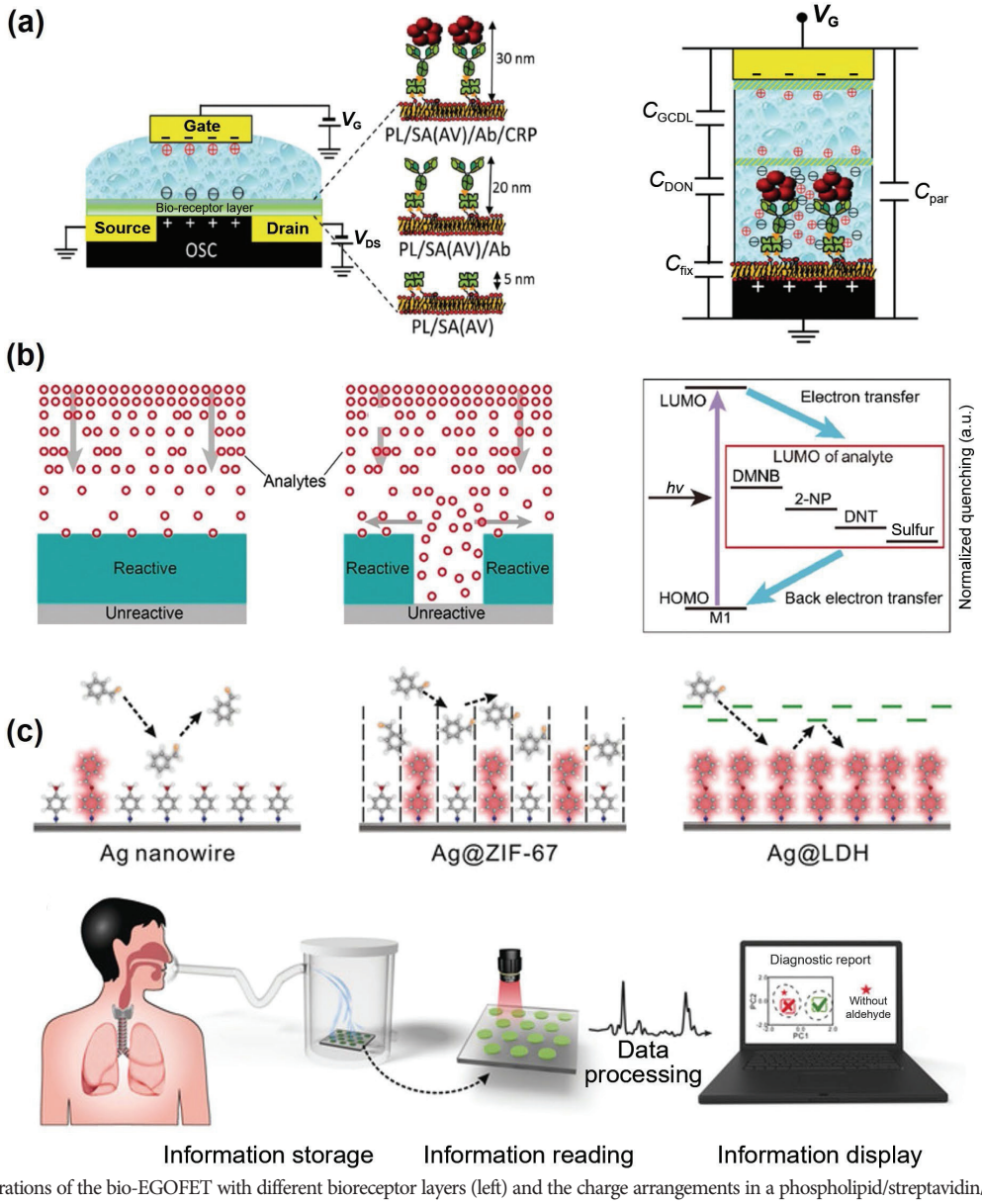

Figure 12 (a) Illustrations of the bio-EGOFET with different bioreceptor layers (left) and the charge arrangements in a phospholipid/streptavidin/antibody/C-reactive protein (PL/SA/Ab/CRP) multilayer (right). Reproduced with permission from Ref. [99], © WILEY-VCH Verlag GmbH & Co. KGaA, Weinheim 2015. (b) The movements of gas molecules at flat and patterned arrays (left), and the detection mechanism for gas molecules such as 2,4-dinitrotoluene (DNT), 2-nitrophenol (2-NP), 2,3-dimethyl-2,3-dinitrobutane (DMNB), and sulfur with photoinduced electron transfer (right). Reproduced with permission from Ref. [49], © Wiley-VCH Verlag GmbH & Co. KGaA, Weinheim 2020. (c) The conformational strategy transition of the analyte with a substrate for determining VOCs. Reproduced with permission from Ref. [103], © Wiley-VCH Verlag GmbH & Co. KGaA, Weinheim 2019.

synaptic behaviors but also mimics the parallel signal processing and transmissions in biological multipolar neurons. The proposed MoS_2 tactile synaptic transistor exhibited a broad application in intelligent human–computer interactions. As for neural networks based on synapses, low energy consumption (voltage and current) should be considered carefully in the practical applications of bionic electronics. Shi et al. [111] demonstrated an artificial optic-neural network made from an 8 × 8 fully solution-printed-photo synaptic OFET (FSP-OFET) array with reduced energy consumption in Fig. 14(e), which lowered the working voltage and current and provided the capability to emulate visual nervous responses to external light stimuli with ultralow energy consumption (0.07–34 and 0.41–19.87 fJ per spike in short-term and long-term plasticity, respectively).

7 Conclusion and perspective

Currently, OTFT-based biosensors have been applied to the real-time recognition of target analytes in the environment, providing a convenient and noninvasive method for rapid and immediate clinical treatment and health monitoring [112–116]. Compared with other sensing methods, OTFT-based biosensor has many advantages: (1) OTFTs are biocompatible for label-free detection with both signal conversion and amplification characteristics, which can cause changes in charge concentration through specific biochemical reactions. (2) OTFTs are simple in construction and low-cost in production cost, which can significantly simplify the experimental process and facilitate batch production. (3) OTFTs are easy to be miniaturized and integrated into the circuit for simultaneous detection of different biomarkers with high reliability.

Nevertheless, challenges in developing OTFTs still need to be addressed: (1) It remains challenging to obtain new OSC materials with both high stability and high sensitivity, thus limiting their extended future applications. (2) A fundamental understanding of the sensing mechanism needs to be further enhanced, particularly

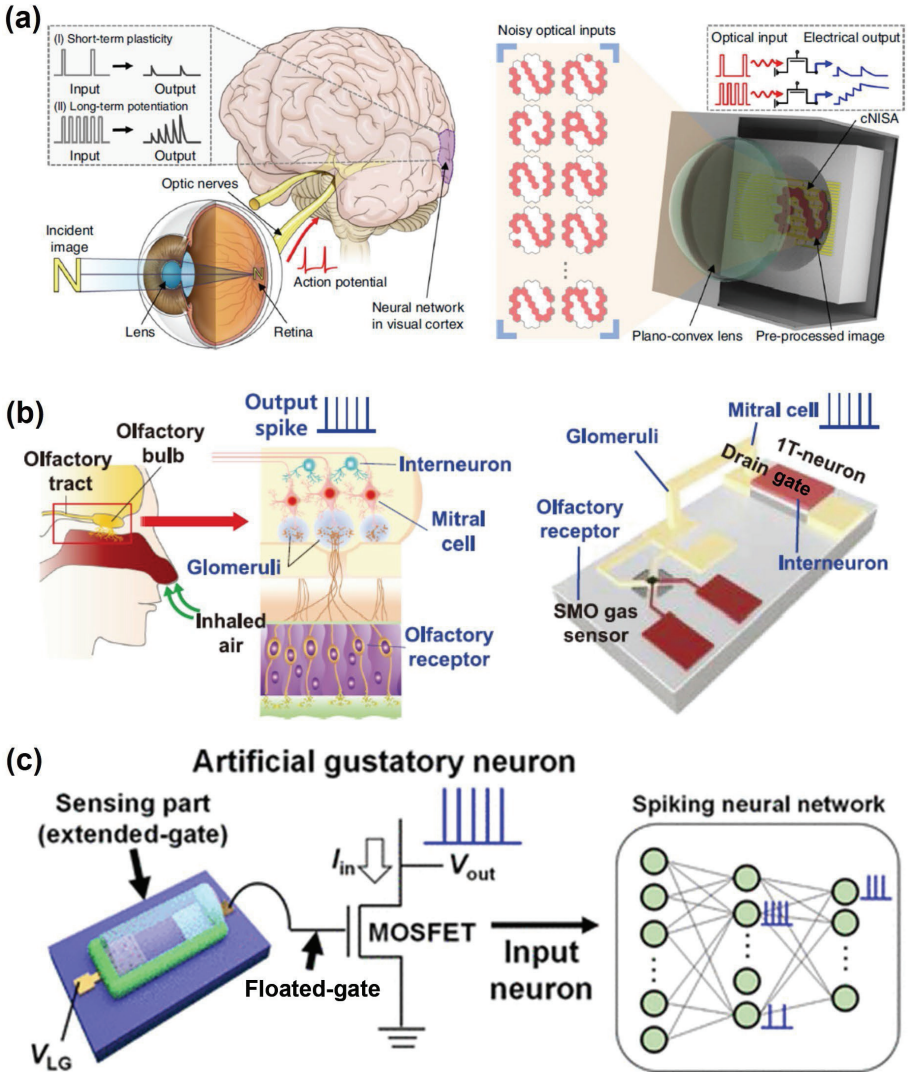

Figure 13 (a) Illustrations of the human visual recognition system (left) and the curved neuromorphic imaging device (right). Reproduced with permission from Ref. [106], © Choi, C. et al. 2020. (b) Illustrations of the biological olfactory system composed of various olfactory neurons (left), and the artificial olfactory neuron module composed of an SMO gas sensor and an MOSFET-based 1T-neuron (right). Reproduced with permission from Ref. [107], © Han, J. K. et al. 2022. (c) Illustration of the artificial gustatory neuron based on a spiking neural network. Reproduced with permission from Ref. [108], © American Chemical Society 2022.

how the different target analytes affect the transportation of charge carriers. (3) Improve the reusability of OTFT-based bioassay through specific optimization strategies, which can further decrease the cost of preparation. (4) Self-powered OTFT-based sensor by solar cell will promote the point-of-care diagnosis at home without professional testers. (5) Integrating with other technologies can make full use of the advantages of OTFT-based sensors in health monitoring with enhanced reliability.

With the rapid development of science and technology, how to achieve high-effective OTFT-based biosensor has attracted significant attention in recent years. Ideally, bio-electronic systems require conformal contact between active materials and organisms to connect biology and the digital world. Therefore, improvements in materials and technologies will be the key to achieving a high-effective OTFT-based biosensor array in life and health monitoring. From the perspective of materials: (1) Optimize the sensing layer thickness, morphology, and microstructure of the OSCs for target molecules; (2) modify specific functional groups on OSCs for specific identification of antibodies, enzymes, aptamers, and artificial protein receptors; (3) introduce porous structures on the OSCs to integrate the receptor materials into OTFT-based biosensors. From the perspective of technologies: (1) Fabricate large-area OSCs with homogeneous properties, such as controlled orientation, crystal uniformity, and thickness; (2) achieving miniaturization and intelligence is an essential direction for precise quantification and recognition of target analytes based on OTFTs; (3) improve the ability to output a stable and repeatable signal during repeated operations by encapsulation or optimization in the preparation process.

OTFT-based biosensor, as an advanced and effective method for biochemical analysis, is a combination of chemistry, materials, life, and microelectronics technologies. Accompanied by the rapid development of OTFTs with other technologies, bioelectronics will provide more opportunities to achieve high-throughput screening of biomarkers in complex solution media, which will be beneficial to push OTFT-based sensing technology into clinical diagnosis.

Acknowledgments

This work was financially supported by the National Natural Science Foundation of China (Nos. 21925405, 22104141, 22104142, 22004122, and 201874005), the National Key Research and Development Program of China Grant (Nos. 2018YFA0208800 and 2021YFD1700300), the Chinese Academy of Sciences (Nos. XDA23030106 and YJKYYQ20180044), and the China Postdoctoral Science Foundation (Nos. 2020M680676 and 2021T140680).

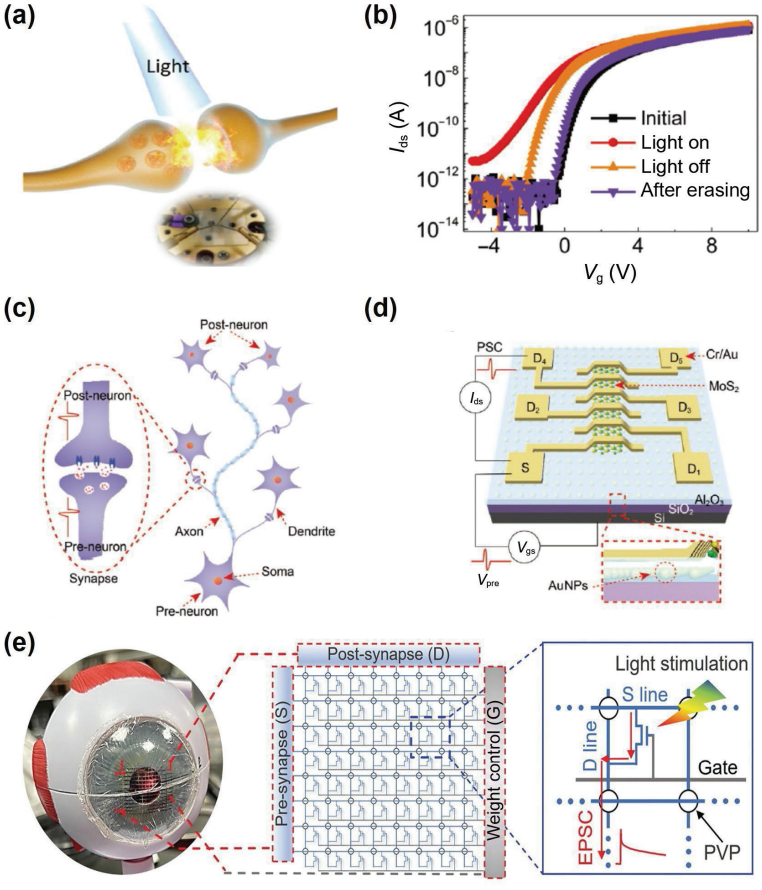

Figure 14 (a) Illustration of the biological synapse based on a stretchable MoS_2 device. (b) Transfer curves of the device at the states of initial (black), light on (red), light off (orange), and after erasing (purple), respectively. Reproduced with permission from Ref. [109], © Wiley-VCH GmbH 2022. (c) Illustration of the biological multipolar neuron. (d) Structure of multi-terminal MoS_2 synaptic transistor. Reproduced with permission from Ref. [110], © Mo, W. A. et al. 2022. (e) Image of the proposed photo synaptic array based on FSP-OFET attached on the eyeball model. Reproduced with permission from Ref. [111], © Wiley-VCH GmbH 2022.

References

[1] Luo, X. L.; Davis, J. J. Electrical biosensors and the label free detection of protein disease biomarkers. *Chem. Soc. Rev.* **2013**, *42*, 5944–5962.

[2] Wang, C. L.; Dong, H. L.; Hu, W. P.; Liu, Y. Q.; Zhu, D. B. Semiconducting π-conjugated systems in field-effect transistors: A material odyssey of organic electronics. *Chem. Rev.* **2012**, *112*, 2208–2267.

[3] Rivnay, J.; Inal, S.; Salleo, A.; Owens, R. M.; Berggren, M.; Malliaras, G. G. Organic electrochemical transistors. *Nat. Rev. Mater.* **2018**, *3*, 17086.

[4] Zhang, C. C.; Chen, P. L.; Hu, W. P. Organic field-effect transistor-based gas sensors. *Chem. Soc. Rev.* **2015**, *44*, 2087–2107.

[5] Li, H.; Shi, W.; Song, J.; Jang, H. J.; Dailey, J.; Yu, J. S.; Katz, H. E. Chemical and biomolecule sensing with organic field-effect transistors. *Chem. Rev.* **2019**, *119*, 3–35.

[6] Wang, Y. J.; Gong, Q.; Miao, Q. Structured and functionalized organic semiconductors for chemical and biological sensors based on organic field effect transistors. *Mater. Chem. Front.* **2020**, *4*, 3505–3520.

[7] Wang, N. X.; Yang, A. N.; Fu, Y.; Li, Y. Z.; Yan, F. Functionalized organic thin film transistors for biosensing. *Acc. Chem. Res.* **2019**, *52*, 277–287.

[8] Macchia, E.; De Caro, L.; Torricelli, F.; Franco, C. D.; Mangiatordi, G. F.; Scamarcio, G.; Torsi, L. Why a diffusing single-molecule can be detected in few minutes by a large capturing bioelectronic interface. *Adv. Sci.* **2022**, *9*, 2104381.

[9] Macchia, E.; Tiwari, A.; Manoli, K.; Holzer, B.; Ditaranto, N.; Picca, R. A.; Cioffi, N.; Di Franco, C.; Scamarcio, G.; Palazzo, G. et al. Label-free and selective single-molecule bioelectronic sensing with a millimeter-wide self-assembled monolayer of anti-immunoglobulins. *Chem. Mater.* **2019**, *31*, 6476–6483.

[10] Tang, W.; Fu, Y.; Huang, Y. K.; Li, Y. Z.; Song, Y. W.; Xi, X.; Yu, Y. D.; Su, Y. Z.; Yan, F.; Guo, X. J. Solution processed low power organic field-effect transistor bio-chemical sensor of high transconductance efficiency. *npj Flex. Electron.* **2022**, *6*, 18.

[11] Dai, C. H.; Liu, Y. Q.; Wei, D. C. Two-dimensional field-effect transistor sensors: The road toward commercialization. *Chem. Rev.* **2022**, *122*, 10319–10392.

[12] Jang, Y.; Jang, M.; Kim, H.; Lee, S. J.; Jin, E.; Koo, J. Y.; Hwang, I. C.; Kim, Y.; Ko, Y. H.; Hwang, I. et al. Point-of-use detection of amphetamine-type stimulants with host-molecule-functionalized organic transistors. *Chem* **2017**, *3*, 641–651.

[13] Decataldo, F.; Barbalinardo, M.; Gentili, D.; Tessarolo, M.; Calienni, M.; Cavallini, M.; Fraboni, B. Organic electrochemical transistors for real-time monitoring of *in vitro* silver nanoparticle toxicity. *Adv. Biosys.* **2020**, *4*, 1900204.

[14] Zhang, Y. P.; Kuang, J. H.; Dong, J. C.; Shi, L. X.; Li, Q. Y.; Zhang, B. J.; Shi, W.; Huang, X.; Zhu, Z. H.; Ma, Y. Q. et al. Ultra-sensitive boscalid sensors based on a β-cyclodextrin modified perfluorinated copper phthalocyanine field-effect transistor. *J. Mater. Chem. C* **2021**, *9*, 12877–12883.

[15] Zhou, X. Y.; Xue, Z. J.; Wang, T. A point-of-care biosensor for rapid and ultra-sensitive detection of SARS-CoV-2. *Matter* **2022**, *5*, 2402–2404.

[16] Wang, L. Q.; Wang, X. J.; Wu, Y. G.; Guo, M. Q.; Gu, C. J.; Dai, C. H.; Kong, D. R.; Wang, Y.; Zhang, C.; Qu, D. et al. Rapid and ultrasensitive electromechanical detection of ions, biomolecules, and SARS-CoV-2 RNA in unamplified samples. *Nat. Biomed. Eng.* **2022**, *6*, 276–285.

[17] Novodchuk, I.; Kayaharman, M.; Prassas, I.; Soosaipillai, A.; Karimi, R.; Goldthorpe, I. A.; Abdel-Rahman, E.; Sanderson, J.; Diamandis, E. P.; Bajcsy, M. et al. Electronic field effect detection of SARS-CoV-2 N-protein before the onset of symptoms. *Biosens. Bioelectron.* **2022**, *210*, 114331.

[18] Gwyther, R. E. A.; Nekrasov, N. P.; Emelianov, A. V.; Nasibulin, A. G.; Ramakrishnan, K.; Bobrinetskiy, I.; Jones, D. D. Differential bio-optoelectronic gating of semiconducting carbon nanotubes by varying the covalent attachment residue of a green fluorescent protein. *Adv. Funct. Mater.* **2022**, *32*, 2112374.
[19] Bonafè, F.; Decataldo, F.; Zironi, I.; Remondini, D.; Cramer, T.; Fraboni, B. AC amplification gain in organic electrochemical transistors for impedance-based single cell sensors. *Nat. Commun.* **2022**, *13*, 5423.
[20] Guo, X.; Cao, Q. Q.; Liu, Y. W.; He, T.; Liu, J. W.; Huang, S.; Tang, H.; Ma, M. Organic electrochemical transistor for *in situ* detection of H_2O_2 released from adherent cells and its application in evaluating the *in vitro* cytotoxicity of nanomaterial. *Anal. Chem.* **2020**, *92*, 908–915.
[21] Tsumura, A.; Koezuka, H.; Ando, T. Macromolecular electronic device: Field-effect transistor with a polythiophene thin film. *Appl. Phys. Lett.* **1986**, *49*, 1210–1212.
[22] Sun, C. F.; Wang, X.; Auwalu, M. A.; Cheng, S. S.; Hu, W. P. Organic thin film transistors-based biosensors. *EcoMat* **2021**, *3*, e12094.
[23] Someya, T.; Dodabalapur, A.; Huang, J.; See, K. C.; Katz, H. E. Chemical and physical sensing by organic field-effect transistors and related devices. *Adv. Mater.* **2010**, *22*, 3799–3811.
[24] Kim, S. H.; Hong, K.; Xie, W.; Lee, K. H.; Zhang, S. P.; Lodge, T. P.; Frisbie, C. D. Electrolyte-gated transistors for organic and printed electronics. *Adv. Mater.* **2013**, *25*, 1822–1846.
[25] Sun, C. F.; Wang, Y. X.; Sun, M. Y.; Zou, Y.; Zhang, C. C.; Cheng, S. S.; Hu, W. P. Facile and cost-effective liver cancer diagnosis by water-gated organic field-effect transistors. *Biosens. Bioelectron.* **2020**, *164*, 112251.
[26] Liao, C. Z.; Zhang, M.; Yao, M. Y.; Hua, T.; Li, L.; Yan, F. Flexible organic electronics in biology: Materials and devices. *Adv. Mater.* **2015**, *27*, 7493–7527.
[27] Huang, J.; Miragliotta, J.; Becknell, A.; Katz, H. E. Hydroxy-terminated organic semiconductor-based field-effect transistors for phosphonate vapor detection. *J. Am. Chem. Soc.* **2007**, *129*, 9366–9376.
[28] Liu, D. P.; Chu, Y. L.; Wu, X. H.; Huang, J. Side-chain effect of organic semiconductors in OFET-based chemical sensors. *Sci. China Mater.* **2017**, *60*, 977–984.
[29] Xu, J.; Wang, S. H.; Wang, G. J. N.; Zhu, C. X.; Luo, S. C.; Jin, L. H.; Gu, X. D.; Chen, S. C.; Feig, V. R.; To, J. W. F. et al. Highly stretchable polymer semiconductor films through the nanoconfinement effect. *Science* **2017**, *355*, 59–64.
[30] Paterson, A. F.; Savva, A.; Wustoni, S.; Tsetseris, L.; Paulsen, B. D.; Faber, H.; Emwas, A. H.; Chen, X. X.; Nikiforidis, G.; Hidalgo, T. C. et al. Water stable molecular n-doping produces organic electrochemical transistors with high transconductance and record stability. *Nat. Commun.* **2020**, *11*, 3004.
[31] Iskierko, Z.; Noworyta, K.; Sharma, P. S. Molecular recognition by synthetic receptors: Application in field-effect transistor based chemosensing. *Biosens. Bioelectron.* **2018**, *109*, 50–62.
[32] Whitcombe, M. J.; Chianella, I.; Larcombe, L.; Piletsky, S. A.; Noble, J.; Porter, R.; Horgan, A. The rational development of molecularly imprinted polymer-based sensors for protein detection. *Chem. Soc. Rev.* **2011**, *40*, 1547–1571.
[33] Zhou, Q.; Wang, M. Q.; Yagi, S.; Minami, T. Extended gate-type organic transistor functionalized by molecularly imprinted polymer for taurine detection. *Nanoscale* **2021**, *13*, 100–107.
[34] Dai, C. H.; Guo, M. Q.; Wu, Y. L.; Cao, B. P.; Wang, X. J.; Wu, Y. G.; Kang, H.; Kong, D. R.; Zhu, Z. Q.; Ying, T. L. et al. Ultraprecise antigen 10-in-1 pool testing by multiantibodies transistor assay. *J. Am. Chem. Soc.* **2021**, *143*, 19794–19801.
[35] Di, C. A.; Liu, Y. Q.; Yu, G.; Zhu, D. B. Interface engineering: An effective approach toward high-performance organic field-effect transistors. *Acc. Chem. Res.* **2009**, *42*, 1573–1583.
[36] Ji, D. Y.; Li, L. Q.; Fuchs, H.; Hu, W. P. Engineering the interfacial materials of organic field-effect transistors for efficient charge transport. *Acc. Mater. Res.* **2021**, *2*, 159–169.
[37] Chen, H. L.; Zhang, W. N.; Li, M. L.; He, G.; Guo, X. F. Interface engineering in organic field-effect transistors: Principles, applications, and perspectives. *Chem. Rev.* **2020**, *120*, 2879–2949.
[38] Wang, S. Y.; Zhao, X. L.; Zhang, C.; Yang, Y. H.; Liang, J.; Ni, Y. P.; Zhang, M. X.; Li, J. T.; Ye, X. L.; Zhang, J. D. et al. Suppressing interface strain for eliminating double-slope behaviors: Towards ideal conformable polymer field-effect transistors. *Adv. Mater.* **2021**, *33*, 2101633.
[39] Zhang, K.; Kotadiya, N. B.; Wang, X. Y.; Wetzelaer, G. J. A. H.; Marszalek, T.; Pisula, W.; Blom, P. W. M. Interlayers for improved hole injection in organic field-effect transistors. *Adv. Electron. Mater.* **2020**, *6*, 1901352.
[40] Huang, J.; Du, J.; Cevher, Z.; Ren, Y. H.; Wu, X. H.; Chu, Y. L. Printable and flexible phototransistors based on blend of organic semiconductor and biopolymer. *Adv. Funct. Mater.* **2017**, *27*, 1604163.
[41] Zhang, Y. P.; Liu, X. T.; Qiu, S.; Zhang, Q. Q.; Tang, W.; Liu, H. T.; Guo, Y. L.; Ma, Y. Q.; Guo, X. J.; Liu, Y. Q. A flexible acetylcholinesterase-modified graphene for chiral pesticide sensor. *J. Am. Chem. Soc.* **2019**, *141*, 14643–14649.
[42] Duan, S. M.; Wang, T.; Geng, B. W.; Gao, X.; Li, C. G.; Zhang, J.; Xi, Y.; Zhang, X. T.; Ren, X. C.; Hu, W. P. Solution-processed centimeter-scale highly aligned organic crystalline arrays for high-performance organic field-effect transistors. *Adv. Mater.* **2020**, *32*, 1908388.
[43] Ren, H.; Cui, N.; Tang, Q. X.; Tong, Y. H.; Zhao, X. L.; Liu, Y. C. High-performance, ultrathin, ultraflexible organic thin-film transistor array via solution process. *Small* **2018**, *14*, 1801020.
[44] Yang, Y. B.; Wang, J. F.; Huang, W. T.; Wan, G. J.; Xia, M. M.; Chen, D.; Zhang, Y.; Wang, Y. M.; Guo, F. D.; Tan, J. et al. Integrated urinalysis devices based on interface-engineered field-effect transistor biosensors incorporated with electronic circuits. *Adv. Mater.* **2022**, *34*, 2203224.
[45] Anisimov, D. S.; Chekusova, V. P.; Trul, A. A.; Abramov, A. A.; Borshchev, O. V.; Agina, E. V.; Ponomarenko, S. A. Fully integrated ultra-sensitive electronic nose based on organic field-effect transistors. *Sci. Rep.* **2021**, *11*, 10683.
[46] Wang, T. T.; Ma, S. Q.; Lv, A. F.; Liu, F. J.; Yin, X. B. Concentration recognition of gas sensor with organic field-effect transistor assisted by artificial intelligence. *Sens. Actuators B: Chem.* **2022**, *363*, 131854.
[47] Lu, J. J.; Liu, D. P.; Zhou, J. C.; Chu, Y. L.; Chen, Y. T.; Wu, X. H.; Huang, J. Porous organic field-effect transistors for enhanced chemical sensing performances. *Adv. Funct. Mater.* **2017**, *27*, 1700018.
[48] Yuvaraja, S.; Surya, S. G.; Chernikova, V.; Vijjapu, M. T.; Shekhah, O.; Bhatt, P. M.; Chandra, S.; Eddaoudi, M.; Salama, K. N. Realization of an ultrasensitive and highly selective OFET NO_2 sensor: The synergistic combination of PDVT-10 polymer and porphyrin-MOF. *ACS Appl. Mater. Interfaces* **2020**, *12*, 18748–18760.
[49] Liu, L.; Xiong, W.; Cui, L. F.; Xue, Z. J.; Huang, C. H.; Song, Q.; Bai, W. Q.; Peng, Y. G.; Chen, X. Y.; Liu, K. Y. et al. Universal strategy for improving the sensitivity of detecting volatile organic compounds by patterned arrays. *Angew. Chem., Int. Ed.* **2020**, *59*, 15953–15957.
[50] Seshadri, P.; Manoli, K.; Schneiderhan-Marra, N.; Anthes, U.; Wierzchowiec, P.; Bonrad, K.; Di Franco, C.; Torsi, L. Low-picomolar, label-free procalcitonin analytical detection with an electrolyte-gated organic field-effect transistor based electronic immunosensor. *Biosens. Bioelectron.* **2018**, *104*, 113–119.
[51] Buth, F.; Donner, A.; Sachsenhauser, M.; Stutzmann, M.; Garrido, J. A. Biofunctional electrolyte-gated organic field-effect transistors. *Adv. Mater.* **2012**, *24*, 4511–4517.
[52] Minamiki, T.; Sasaki, Y.; Tokito, S.; Minami, T. Label-free direct electrical detection of a histidine-rich protein with sub-femtomolar sensitivity using an organic field-effect transistor. *ChemistryOpen* **2017**, *6*, 472–475.
[53] Kim, D. J.; Lee, N. E.; Park, J. S.; Park, I. J.; Kim, J. G.; Cho, H. J. Organic electrochemical transistor based immunosensor for prostate specific antigen (PSA) detection using gold nanoparticles for signal amplification. *Biosens. Bioelectron.* **2010**, *25*, 2477–2482.
[54] Shen, H. G.; Zou, Y.; Zang, Y. P.; Huang, D. Z.; Jin, W. L.; Di, C.

A.; Zhu, D. B. Molecular antenna tailored organic thin-film transistors for sensing application. *Mater. Horiz.* **2018**, *5*, 240–247.
[55] Iqbal, H. F.; Ai, Q. X.; Thorley, K. J.; Chen, H.; McCulloch, I.; Risko, C.; Anthony, J. E.; Jurchescu, O. D. Suppressing bias stress degradation in high performance solution processed organic transistors operating in air. *Nat. Commun.* **2021**, *12*, 2352.
[56] Nikolka, M.; Nasrallah, I.; Rose, B.; Ravva, M. K.; Broch, K.; Sadhanala, A.; Harkin, D.; Charmet, J.; Hurhangee, M.; Brown, A. et al. High operational and environmental stability of high-mobility conjugated polymer field-effect transistors through the use of molecular additives. *Nat. Mater.* **2017**, *16*, 356–362.
[57] Simatos, D.; Spalek, L. J.; Kraft, U.; Nikolka, M.; Jiao, X.; McNeill, C. R.; Venkateshvaran, D.; Sirringhaus, H. The effect of the dielectric end groups on the positive bias stress stability of N2200 organic field effect transistors. *APL Mater.* **2021**, *9*, 041113.
[58] Jia, X. J.; Fuentes-Hernandez, C.; Wang, C. Y.; Park, Y.; Kippelen, B. Stable organic thin-film transistors. *Sci. Adv.* **2018**, *4*, eaao1705.
[59] Zhai, C. Y.; Yang, X. H.; Han, S. Y.; Lu, G. H.; Wei, P.; Chumakov, A.; Erbes, E.; Chen, Q.; Techert, S.; Roth, S. V. et al. Surface etching of polymeric semiconductor films improves environmental stability of transistors. *Chem. Mater.* **2021**, *33*, 2673–2682.
[60] Sun, C. F.; Li, R.; Song, Y. R.; Jiang, X. Q.; Zhang, C. C.; Cheng, S. S.; Hu, W. P. Ultrasensitive and reliable organic field-effect transistor-based biosensors in early liver cancer diagnosis. *Anal. Chem.* **2021**, *93*, 6188–6194.
[61] Sun, C. F.; Vinayak, M. V.; Cheng, S. S.; Hu, W. P. Facile functionalization strategy for ultrasensitive organic protein biochips in multi-biomarker determination. *Anal. Chem.* **2021**, *93*, 11305–11311.
[62] Sun, C. F.; Feng, G. Y.; Song, Y. R.; Cheng, S. S.; Lei, S. B.; Hu, W. P. Single molecule level and label-free determination of multibiomarkers with an organic field-effect transistor platform in early cancer diagnosis. *Anal. Chem.* **2022**, *94*, 6615–6620.
[63] Li, P. H.; Jia, C. C.; Guo, X. F. Molecule-based transistors: From macroscale to single molecule. *Chem. Rec.* **2021**, *21*, 1284–1299.
[64] Macchia, E.; Manoli, K.; Holzer, B.; Di Franco, C.; Ghittorelli, M.; Torricelli, F.; Alberga, D.; Mangiatordi, G. F.; Palazzo, G.; Scamarcio, G. et al. Single-molecule detection with a millimetre-sized transistor. *Nat. Commun.* **2018**, *9*, 3223.
[65] Bai, J.; Li, X. H.; Zhu, Z. Y.; Zheng, Y.; Hong, W. J. Single-molecule electrochemical transistors. *Adv. Mater.* **2021**, *33*, 2005883.
[66] Guo, K. Y.; Wustoni, S.; Koklu, A.; Díaz-Galicia, E.; Moser, M.; Hama, A.; Alqahtani, A. A.; Ahmad, A. N.; Alhamlan, F. S.; Shuaib, M. et al. Rapid single-molecule detection of COVID-19 and MERS antigens via nanobody-functionalized organic electrochemical transistors. *Nat. Biomed. Eng.* **2021**, *5*, 666–677.
[67] Koklu, A.; Wustoni, S.; Guo, K. Y.; Silva, R.; Salvigni, L.; Hama, A.; Diaz-Galicia, E.; Moser, M.; Marks, A.; McCulloch, I. et al. Convection driven ultrarapid protein detection via nanobody-functionalized organic electrochemical transistors. *Adv. Mater.* **2022**, *34*, 2202972.
[68] Liu, H.; Yang, A. N.; Song, J. J.; Wang, N. X.; Lam, P.; Li, Y.; Law, H. K. W.; Yan, F. Ultrafast, sensitive, and portable detection of COVID-19 IgG using flexible organic electrochemical transistors. *Sci. Adv.* **2021**, *7*, eabg8387.
[69] Zhang, T.; Deng, R. J.; Wang, Y. X.; Wu, C. Y.; Zhang, K. X.; Wang, C. Y.; Gong, N. Q.; Ledesma-Amaro, R.; Teng, X. C.; Yang, C. R. et al. A paper-based assay for the colorimetric detection of SARS-CoV-2 variants at single-nucleotide resolution. *Nat. Biomed. Eng.* **2022**, *6*, 957–967.
[70] Stoliar, P.; Bystrenova, E.; Quiroga, S. D.; Annibale, P.; Facchini, M.; Spijkman, M.; Setayesh, S.; de Leeuw, D.; Biscarini, F. DNA adsorption measured with ultra-thin film organic field effect transistors. *Biosens. Bioelectron.* **2009**, *24*, 2935–2938.
[71] Kim, J. M.; Jha, S. K.; Chand, R.; Lee, D. H.; Kim, Y. S. DNA hybridization sensor based on pentacene thin film transistor. *Biosens. Bioelectron.* **2011**, *26*, 2264–2269.
[72] Demelas, M.; Lai, S.; Casula, G.; Scavetta, E.; Barbaro, M.; Bonfiglio, A. An organic, charge-modulated field effect transistor for DNA detection. *Sens. Actuators B: Chem* **2012**, *171–172*, 198–203.
[73] Sun, M. Y.; Zhang, C. C.; Wang, J.; Sun, C. F.; Ji, Y. C.; Cheng, S. S.; Liu, H. Construction of high stable all-graphene-based FETs as highly sensitive dual-signal miRNA sensors by a covalent layer-by-layer assembling method. *Adv. Electron. Mater.* **2020**, *6*, 2000731.
[74] Macchia, E.; Manoli, K.; Di Franco, C.; Picca, R. A.; Österbacka, R.; Palazzo, G.; Torricelli, F.; Scamarcio, G.; Torsi, L. Organic field-effect transistor platform for label-free, single-molecule detection of genomic biomarkers. *ACS Sens.* **2020**, *5*, 1822–1830.
[75] Gao, J. W.; Gao, Y. K.; Han, Y. K.; Pang, J. B.; Wang, C.; Wang, Y. H.; Liu, H.; Zhang, Y.; Han, L. Ultrasensitive label-free miRNA sensing based on a flexible graphene field-effect transistor without functionalization. *ACS Appl. Electron. Mater.* **2020**, *2*, 1090–1098.
[76] Sun, M. Y.; Zhang, C. C.; Chen, D.; Wang, J.; Ji, Y. C.; Liang, N.; Gao, H. Y.; Cheng, S. S.; Liu, H. Ultrasensitive and stable all graphene field-effect transistor-based Hg^{2+} sensor constructed by using different covalently bonded RGO films assembled by different conjugate linking molecules. *SmartMat* **2021**, *2*, 213–225.
[77] Ji, X. D.; Lau, H. Y.; Ren, X. C.; Peng, B. Y.; Zhai, P.; Feng, S. P.; Chan, P. K. L. Highly sensitive metabolite biosensor based on organic electrochemical transistor integrated with microfluidic channel and poly(N-vinyl-2-pyrrolidone)-capped platinum nanoparticles. *Adv. Mater. Technol.* **2016**, *1*, 1600042.
[78] Shi, W.; Li, Q. Y.; Zhang, Y. P.; Liu, K.; Huang, X.; Yang, X. L.; Ran, Y.; Li, Y. F.; Guo, Y. L.; Liu, Y. Q. Enabling the aqueous solution sensing of skin-conformable organic field-effect transistor using an amphiphilic molecule. *Appl. Mater. Today* **2022**, *26*, 101275.
[79] Liao, C. Z.; Zhang, M.; Niu, L. Y.; Zheng, Z. J.; Yan, F. Highly selective and sensitive glucose sensors based on organic electrochemical transistors with graphene-modified gate electrodes. *J. Mater. Chem. B* **2013**, *1*, 3820–3829.
[80] Currano, L. J.; Sage, F. C.; Hagedon, M.; Hamilton, L.; Patrone, J.; Gerasopoulos, K. Wearable sensor system for detection of lactate in sweat. *Sci. Rep.* **2018**, *8*, 15890.
[81] Minami, T.; Sato, T.; Minamiki, T.; Fukuda, K.; Kumaki, D.; Tokito, S. A novel OFET-based biosensor for the selective and sensitive detection of lactate levels. *Biosens. Bioelectron.* **2015**, *74*, 45–48.
[82] Jackowska, K.; Krysinski, P. New trends in the electrochemical sensing of dopamine. *Anal. Bioanal. Chem.* **2013**, *405*, 3753–3771.
[83] Liao, C. Z.; Zhang, M.; Niu, L. Y.; Zheng, Z. J.; Yan, F. Organic electrochemical transistors with graphene-modified gate electrodes for highly sensitive and selective dopamine sensors. *J. Mater. Chem. B* **2014**, *2*, 191–200.
[84] Song, J. J.; Zheng, J. Z.; Yang, A. N.; Liu, H.; Zhao, Z. Y.; Wang, N. X.; Yan, F. Metal–organic framework transistors for dopamine sensing. *Mater. Chem. Front.* **2021**, *5*, 3422–3427.
[85] Ferro, L. M. M.; Merces, L.; de Camargo, D. H. S.; Bof Bufon, C. C. Ultrahigh-gain organic electrochemical transistor chemosensors based on self-curled nanomembranes. *Adv. Mater.* **2021**, *33*, 2101518.
[86] Wang, B.; Zhao, C. Z.; Wang, Z. Q.; Yang, K. A.; Cheng, X. B.; Liu, W. F.; Yu, W. Z.; Lin, S. Y.; Zhao, Y. C.; Cheung, K. M. et al. Wearable aptamer-field-effect transistor sensing system for noninvasive cortisol monitoring. *Sci. Adv.* **2022**, *8*, eabk0967.
[87] Jeong, G.; Oh, J.; Jang, J. Fabrication of N-doped multidimensional carbon nanofibers for high-performance cortisol biosensors. *Biosens. Bioelectron.* **2019**, *131*, 30–36.
[88] Woo, K.; Kang, W.; Lee, K.; Lee, P.; Kim, Y.; Yoon, T. S.; Cho, C. Y.; Park, K. H.; Ha, M. W.; Lee, H. H. Enhancement of cortisol measurement sensitivity by laser illumination for AlGaN/GaN transistor biosensor. *Biosens. Bioelectron.* **2020**, *159*, 112186.
[89] Aerathupalathu Janardhanan, J.; Chen, Y. L.; Liu, C. T.; Tseng, H. S.; Wu, P. I.; She, J. W.; Hsiao, Y. S.; Yu, H. H. Sensitive detection of sweat cortisol using an organic electrochemical transistor featuring nanostructured poly(3,4-ethylenedioxythiophene) derivatives in the channel layer. *Anal. Chem.* **2022**, *94*, 7584–7593.
[90] Tang, W. X.; Yin, L.; Sempionatto, J. R.; Moon, J. M.; Teymourian, H.; Wang, J. Touch-based stressless cortisol sensing.

Adv. Mater. **2021**, *33*, 2008465.
[91] Zang, Y. P.; Zhang, F. J.; Huang, D. Z.; Di, C. A.; Meng, Q.; Gao, X. K.; Zhu, D. B. Specific and reproducible gas sensors utilizing gas-phase chemical reaction on organic transistors. *Adv. Mater.* **2014**, *26*, 2862–2867.
[92] Song, R. X.; Zhou, X.; Wang, Z.; Zhu, L. N.; Lu, J.; Xue, D.; Wang, Z. F.; Huang, L. Z.; Chi, L. F. High selective gas sensors based on surface modified polymer transistor. *Org. Electron.* **2021**, *91*, 106083.
[93] Deng, Y. P.; Qi, H.; Ma, Y.; Liu, S. B.; Zhao, M. Y.; Guo, Z. H.; Jie, Y. S.; Zheng, R.; Jing, J. Z.; Chen, K. T. et al. A flexible and highly sensitive organic electrochemical transistor-based biosensor for continuous and wireless nitric oxide detection. *Proc. Natl. Acad. Sci. USA* **2022**, *119*, e2208060119.
[94] Li, H. Y.; Shi, Y. J.; Han, G. C.; Liu, J.; Zhang, J.; Li, C. L.; Liu, J.; Yi, Y. P.; Li, T.; Gao, X. K. et al. Monolayer two-dimensional molecular crystals for an ultrasensitive OFET-based chemical sensor. *Angew. Chem., Int. Ed.* **2020**, *59*, 4380–4384.
[95] Yang, Y.; Zhang, G. X.; Luo, H. W.; Yao, J. J.; Liu, Z. T.; Zhang, D. Q. Highly sensitive thin-film field-effect transistor sensor for ammonia with the DPP-bithiophene conjugated polymer entailing thermally cleavable tert-butoxy groups in the side chains. *ACS Appl. Mater. Interfaces* **2016**, *8*, 3635–3643.
[96] Yang, Y. Z.; Liu, Z. T.; Chen, L. L.; Yao, J. J.; Lin, G. B.; Zhang, X. S.; Zhang, G. X.; Zhang, D. Q. Conjugated semiconducting polymer with thymine groups in the side chains: Charge mobility enhancement and application for selective field-effect transistor sensors toward CO and H_2S. *Chem. Mater.* **2019**, *31*, 1800–1807.
[97] Huang, W. G.; Diallo, A. K.; Dailey, J. L.; Besar, K.; Katz, H. E. Electrochemical processes and mechanistic aspects of field-effect sensors for biomolecules. *J. Mater. Chem. C* **2015**, *3*, 6445–6470.
[98] Chua, J. H.; Chee, R. E.; Agarwal, A.; Wong, S. M.; Zhang, G. J. Label-free electrical detection of cardiac biomarker with complementary metal–oxide semiconductor-compatible silicon nanowire sensor arrays. *Anal. Chem.* **2009**, *81*, 6266–6271.
[99] Palazzo, G.; De Tullio, D.; Magliulo, M.; Mallardi, A.; Intranuovo, F.; Mulla, M. Y.; Favia, P.; Vikholm-Lundin, I.; Torsi, L. Detection beyond Debye's length with an electrolyte-gated organic field-effect transistor. *Adv. Mater.* **2015**, *27*, 911–916.
[100] Kaisti, M. Detection principles of biological and chemical FET sensors. *Biosens. Bioelectron.* **2017**, *98*, 437–448.
[101] Song, J.; Dailey, J.; Li, H.; Jang, H. J.; Zhang, P. F.; Wang, J. T. H.; Everett, A. D.; Katz, H. E. Extended solution gate OFET-based biosensor for label-free glial fibrillary acidic protein detection with polyethylene glycol-containing bioreceptor layer. *Adv. Funct. Mater.* **2017**, *27*, 1606506.
[102] Yu, S. H.; Girma, H. G.; Sim, K. M.; Yoon, S.; Park, J. M.; Kong, H.; Chung, D. S. Polymer-based flexible NO_x sensors with ppb-level detection at room temperature using breath-figure molding. *Nanoscale* **2019**, *11*, 17709–17717.
[103] Qiao, X. Z.; Chen, X. Y.; Huang, C. H.; Li, A. L.; Li, X.; Lu, Z. L.; Wang, T. Detection of exhaled volatile organic compounds improved by hollow nanocages of layered double hydroxide on Ag nanowires. *Angew. Chem., Int. Ed.* **2019**, *58*, 16523–16527.
[104] Huang, X. B.; Zhao, W. D.; Chen, X. Y.; Li, J. M.; Ye, H. C.; Li, C. C.; Yin, X. M.; Zhou, X. Y.; Qiao, X. Z.; Xue, Z. J. et al. Gold nanoparticle-bridge array to improve DNA hybridization efficiency of SERS sensors. *J. Am. Chem. Soc.* **2022**, *144*, 17533–17539.
[105] Zhao, W. D.; Li, J. M.; Xue, Z. J.; Qiao, X. Z.; Li, A. L.; Chen, X. Y.; Feng, Y.; Yang, Z.; Wang, T. A separation-sensing platform performing accurate diagnosis of jaundice in complex biological tear fluids. *Angew. Chem., Int. Ed.* **2022**, *61*, e202205628.
[106] Choi, C.; Leem, J.; Kim, M.; Taqieddin, A.; Cho, C.; Cho, K. W.; Lee, G. J.; Seung, H.; Bae, H. J.; Song, Y. M. et al. Curved neuromorphic image sensor array using a MoS_2-organic heterostructure inspired by the human visual recognition system. *Nat. Commun.* **2020**, *11*, 5934.
[107] Han, J. K.; Kang, M. G.; Jeong, J.; Cho, I.; Yu, J. M.; Yoon, K. J.; Park, I.; Choi, Y. K. Artificial olfactory neuron for an in-sensor neuromorphic nose. *Adv. Sci.* **2022**, *9*, 2106017.
[108] Han, J. K.; Park, S. C.; Yu, J. M.; Ahn, J. H.; Choi, Y. K. A bioinspired artificial gustatory neuron for a neuromorphic based electronic tongue. *Nano Lett.* **2022**, *22*, 5244–5251.
[109] Li, J. W.; Li, N.; Wang, Q. Q.; Wei, Z.; He, C. L.; Shang, D. S.; Guo, Y. T.; Zhang, W. Y.; Tang, J.; Liu, J. Y. et al. Highly stretchable MoS_2-based transistors with opto-synaptic functionalities. *Adv. Electron. Mater.* **2022**, *8*, 2200238.
[110] Mo, W. A.; Ding, G. L.; Nie, Z. H.; Feng, Z. H.; Zhou, K.; Chen, R. S.; Xie, P.; Shang, G.; Han, S. T.; Zhou, Y. Spatiotemporal modulation of plasticity in multi-terminal tactile synaptic transistor. *Adv. Electron. Mater.* **2022**, *9*, 2200733.
[111] Shi, J. L.; Jie, J. S.; Deng, W.; Luo, G.; Fang, X. C.; Xiao, Y. L.; Zhang, Y. J.; Zhang, X. J.; Zhang, X. H. A fully solution-printed photosynaptic transistor array with ultralow energy consumption for artificial-vision neural networks. *Adv. Mater.* **2022**, *34*, 2200380.
[112] Yan, Z. C.; Xu, D.; Lin, Z. Y.; Wang, P. Q.; Cao, B. C.; Ren, H. Y.; Song, F.; Wan, C. Z.; Wang, L. Y.; Zhou, J. X. et al. Highly stretchable van der Waals thin films for adaptable and breathable electronic membranes. *Science* **2022**, *375*, 852–859.
[113] Wang, D. Z.; Lu, L. K.; Zhao, Z. Y.; Zhao, K. P.; Zhao, X. Y.; Pu, C. C.; Li, Y. K.; Xu, P. F.; Chen, X. J.; Guo, Y. L. et al. Large area polymer semiconductor sub-microwire arrays by coaxial focused electrohydrodynamic jet printing for high-performance OFETs. *Nat. Commun.* **2022**, *13*, 6214.
[114] Li, W. Y.; Song, Z. Q.; Kong, H. J.; Chen, M. Q.; Liu, S. J.; Bao, Y.; Ma, Y. M.; Sun, Z. H.; Liu, Z. B.; Wang, W. et al. An integrated wearable self-powered platform for real-time and continuous temperature monitoring. *Nano Energy* **2022**, *104*, 107935.
[115] Xiang, Z. H.; Han, M. D.; Zhang, H. X. Nanomaterials based flexible devices for monitoring and treatment of cardiovascular diseases (CVDs). *Nano Res.*, in press, https://doi.org/10.1007/s12274-022-4551-8.
[116] Zan, P.; Than, A.; Zhang, W. Q.; Cai, H. X.; Zhao, W. T.; Chen, P. Transdermal photothermal-pharmacotherapy to remodel adipose tissue for obesity and metabolic disorders. *ACS Nano* **2022**, *16*, 1813–1825.